



Research Paper

LPS decreases CFTR open probability and mucociliary transport through generation of reactive oxygen species

Do Yeon Cho^{a,b,c,1}, Shaoyan Zhang^{a,b,1}, Ahmed Lazrak^{b,d}, Daniel Skinner^{a,b}, Harrison M. Thompson^a, Jessica Grayson^a, Purushotham Guroji^e, Saurabh Aggarwal^{b,d}, Zsuzsanna Bebok^{b,e}, Steven M. Rowe^{b,e,f,g}, Sadis Matalon^{b,d}, Eric J. Sorscher^h, Bradford A. Woodworth^{a,b,*}

^a Department of Otolaryngology Head & Neck Surgery, University of Alabama at Birmingham, Birmingham, AL, USA

^b Gregory Fleming James Cystic Fibrosis Research Center, University of Alabama at Birmingham, Birmingham, AL, USA

^c Division of Otolaryngology, Department of Surgery, Veterans Affairs, Birmingham, AL, USA

^d Department of Anesthesiology, University of Alabama at Birmingham, Birmingham, AL, USA

^e Department of Cell Developmental and Integrative Biology, University of Alabama at Birmingham, Birmingham, AL, USA

^f Department of Pediatrics, University of Alabama at Birmingham, Birmingham, AL, USA

^g Department of Medicine, University of Alabama at Birmingham, Birmingham, AL, USA

^h Department of Pediatrics, Emory University, Atlanta, GA, USA



ARTICLE INFO

Keywords:

Lipopolysaccharide
Cystic fibrosis transmembrane conductance regulator
Reactive
Oxygen species
Mucociliary transport
Micro optical coherence tomography
Chronic rhinosinusitis

ABSTRACT

Lipopolysaccharide (LPS) serves as the interface between gram-negative bacteria (GNB) and the innate immune response in respiratory epithelial cells (REC). Herein, we describe a novel biological role of LPS that permits GNB to persist in the respiratory tract through inducing CFTR and mucociliary dysfunction. LPS reduced cystic fibrosis transmembrane conductance regulator (CFTR)-mediated short-circuit current in mammalian REC in Ussing chambers and nearly abrogated CFTR single channel activity (defined as forskolin-activated Cl⁻ currents) in patch clamp studies, effects of which were blocked with toll-like receptor (TLR)-4 inhibitor. Unitary conductance and single-channel amplitude of CFTR were unaffected, but open probability and number of active channels were markedly decreased. LPS increased cytoplasmic and mitochondrial reactive oxygen species resulting in CFTR carbonylation. All effects of exposure were eliminated when reduced glutathione was added in the medium along with LPS. Functional microanatomy parameters, including mucociliary transport, in human sinonasal epithelial cells *in vitro* were also decreased, but restored with co-incubation with glutathione or TLR-4 inhibitor. *In vivo* measurements, following application of LPS in the nasal cavities showed significant decreases in transepithelial Cl⁻ secretion as measured by nasal potential difference (NPD) – an effect that was nullified with glutathione and TLR-4 inhibitor. These data provide definitive evidence that LPS-generated reactive intermediates downregulate CFTR function *in vitro* and *in vivo* which results in cystic fibrosis-type disease. Findings have implications for therapeutic approaches intent on stimulating Cl⁻ secretion and/or reducing oxidative stress to decrease the sequelae of GNB airway colonization and infection.

1. Introduction

Chronic rhinosinusitis (CRS) affects 1/8 of the adults in the US population and is responsible for annual costs (direct and indirect) of \$22 billion, comprising 5% of annual healthcare expenditures in the U.S [1,2]. Patients with CRS have an abysmal quality of life and have worse

scores on validated questionnaires for pain and social functioning than those afflicted with congestive heart failure, angina, or chronic obstructive pulmonary disease [3]. CRS patients also experience co-morbid depression at twice the rate of the general public [4] and experience poor sleep and severe fatigue that improves with appropriate intervention [5,6].

Patients with cystic fibrosis (CF) have a prevalence of CRS

* Corresponding author. Department of Otolaryngology – Head and Neck Surgery, University of Alabama at Birmingham, 1155 Faculty Office Tower, 510 20th Street South, Birmingham, AL, 35233, USA.

E-mail address: bwoodworth@uabmc.edu (B.A. Woodworth).

¹ Do-Yeon Cho M.D. and Shaoyan Zhang, Ph.D. contributed equally to this work as first authors.

<https://doi.org/10.1016/j.redox.2021.101998>

Received 23 April 2021; Accepted 26 April 2021

Available online 30 April 2021

2213-2317/© 2021 The Authors.

Published by Elsevier B.V. This is an open access article under the CC BY-NC-ND license

(<http://creativecommons.org/licenses/by-nc-nd/4.0/>).

Abbreviations used:

ASL	airway surface liquid
CRS	chronic rhinosinusitis
CBF	ciliary beat frequency
CF	cystic fibrosis
CFBE	cystic fibrosis bronchoepithelia
CFTR	cystic fibrosis transmembrane conductance regulator
GSH	glutathione sulfhydryl
GNB	gram-negative bacteria
HSNE	human sinonasal epithelia
LPS	lipopolysaccharide
μOCT	micro-optical coherence tomography
MCT	mucociliary transport
MNSE	murine nasal septal epithelia
PCL	periciliary liquid
PBS	phosphate buffered saline
ROS	reactive oxygen species
REC	respiratory epithelial cells
Isc	short-circuit current
TLR4	toll-like receptor-4
WT	wild type

approaching 100%. This autosomal recessive disorder is related to deficiency or dysfunction of the cystic fibrosis transmembrane conductance regulator (CFTR). Normal physiologic functions of respiratory epithelium are tightly linked with transepithelial ion and water transport pathways [7]. CFTR is the primary apical anion channel in the sinonasal epithelium, and its presence is necessary for proper hydration and ionic composition of airway surface liquid (ASL). Mucociliary transport (MCT) decreases when CFTR is dysfunctional or deficient, which slows the clearance of respiratory pathogens [8]. Thus, CFTR deficiency leads to increased susceptibility to airway bacterial infections with ensuing chronic inflammatory sinus disease [9–11]. Importantly, otherwise silent carriers for CFTR mutations are predisposed to CRS, indicating that a slight decrease in CFTR expression confers increased likelihood of a CRS disease phenotype [12,13].

While the genetic mutations in individuals afflicted with CF contribute to the overlying phenotypic expression of the disease, there is now long-standing evidence that wild type (WT) CFTR processing, endocytic recycling, and function can also be markedly inhibited by various environmental insults, including high altitude/hypoxemia, cigarette smoke exposure, inflammation, and infectious agents that can contribute to acquired defects in the mucociliary apparatus [14–17]. Additionally, MCT has been shown to be decreased in non-CF CRS and restored once the sinuses are cleared of infection and inflammation [18, 19]. Infection of the sinuses with gram-negative bacteria (GNB) tends to be particularly intense and recalcitrant to treatment [20,21]. *Pseudomonas aeruginosa* is a GNB that commonly colonizes the sinuses and airways of patients with CF and non-CF CRS [11,22–30]. Because non-CF CRS is accompanied by phenotypic resemblances and has similar GNB to CF CRS, it is prudent to consider acquired defects in CFTR as a propagating disease factor for this population.

Respiratory epithelial cells (REC) lining the mammalian airways are the primary interface between pathogens and the host; and the sinus and nasal surfaces are a crucial site for innate immune responses [31,32]. Once *P. aeruginosa* enters the airways, efficient clearance of the bacteria is dependent upon the recognition of the pathogen, which mounts intracellular signaling pathways responsible for triggering an innate response for host defense [33]. *P. aeruginosa* and other GNB exhibit lipopolysaccharide (LPS) in the cell wall, an intensely pro-inflammatory molecule recognized by the pattern recognition receptor toll-like receptor-4 (TLR4). LPS has several important functions for GNB including

aiding as a permeability barrier between the cell and the environment, preserving structural stability of the membrane, and functioning as a protective barrier against foreign particles (antimicrobial peptides, salts, enzymes, drugs, and toxic heavy metals) [34,35]. LPS is critical to the disease capabilities of pathogens and is released from the outer membrane during infection. LPS is also known to generate reactive oxygen species (ROS) and causes a rapid and dynamic translocation of nuclear transcription factor NF-kappa B [36,37]. Given the universal presence of LPS on GNB and the predominance of *Pseudomonas* in CF disease airway colonization and infection, we hypothesized that LPS-induced ROS generation damages CFTR by oxidative modifications resulting in an acquired CFTR and mucociliary dysfunction previously observed in non-CF CRS patients. Further knowledge regarding the interaction of LPS with respiratory epithelium, which serves as the first line of host airway defense in the upper and lower airway, is critical to develop treatment strategies targeting the impacts of early GNB colonization and infection. The objectives of this study are to identify the mechanisms by which LPS contributes to colonization and persistence in the respiratory tract through the induction of acquired defects in the mucociliary apparatus.

2. Methods

2.1. Cell culture

2.1.1. Primary cell culture

Investigational Animal Care and Use Committee and Institutional Review Board approval was obtained from the University of Alabama at Birmingham prior to the initiation of the study. Animal tissue source for REC culture was procured from the nasal septa of C57BL/6 mice and New Zealand white rabbits. Normal human sinonasal mucosa to grow human sinonasal epithelial cultures (HSNE) was obtained intra-operatively from patients undergoing endoscopic surgery for pituitary tumors, facial trauma, benign sinonasal tumors, or lacrimal obstruction. All subjects provided informed consent and were screened for 32 mutations of CFTR, including the 23 core mutations suggested for population-based CF carrier screening by the American Congress of Obstetricians and Gynecologists and the American College of Medical Genetics (Q-ANALY GENE CFTR COM VAR, Quest Diagnostics) [38]. Patients harboring a mutation were excluded from the study. RECs were dissociated from the tissues and grown on semipermeable support membranes (Costar® Transwell® clear 24-well plate inserts, 0.4-μm pore; Corning Life Sciences, Lowell, MA, USA) submerged in culture medium as previously described [14,39–44]. The media was removed from the monolayers on day 4 after reaching confluence, and the cells fed via the basal chamber. Differentiation and ciliogenesis occurred in all mammalian REC cultures within 10–21 days. Monolayers were utilized for analysis when fully differentiated with widespread ciliogenesis and transepithelial resistances >300 Ω·cm².

2.2. Cystic fibrosis bronchoepithelial (CFBE) cell culture

CFBE41o-cells expressing recombinant human CFTR (CFBE-WT, Accession GSM2985447) or flag-tagged recombinant CFTR (D519 CFBE-CMV-CFTR_WT_901FLAG (UAB-corrected sequence) clone # 7) were cultured as previously described (courtesy of John Kappes, PhD) [45]. Cryopreserved cells were warmed, resuspended in Minimal Essential Media+10% Fetal Bovine Serum, and plated in a flasks. Once 80% confluent, the cells were disassociated using PET™ (Athena Enzyme Systems, Baltimore, MD) and seeded on filters (~cell number) as described above. For patch-clamp analysis, cells were seeded on glass coverslips and grown to 30–40% confluency.

2.3. Transepithelial short-circuit current measurements

All chemicals were purchased from Sigma-Aldrich (St. Louis, Mo.)

unless otherwise stated. Filters were incubated with *P. aeruginosa* LPS (Sigma-Aldrich, St. Louis, Mo.) dissolved in phosphate buffered saline (PBS) or vehicle control solutions. Experiments were performed with concentrations of LPS ranging from 0.1 to 100 $\mu\text{g/ml}$ for dose-response testing with the majority of studies completed using an optimal concentration of 10 $\mu\text{g/ml}$ based on effects in the Ussing chamber. Transwell inserts were mounted in Ussing chambers and bathed with solutions that contained (in mM) 120 NaCl, 25 NaHCO₃, 3.3 KH₂PO₄, 0.8 K₂HPO₄, 1.2 MgCl₂, 1.2 CaCl₂, and 10 glucose at a pH 7.3–7.4 [46]. Bath solutions were stirred vigorously and gassed with a mixture of 95% O₂–5% CO₂ at 37 °C. Short-circuit current (I_{sc}) measurements were obtained by using an epithelial voltage clamp (EM-CSYS-8; Physiologic Instruments, San Diego, CA). All experiments were conducted with low Cl⁻ (6 mM) in the mucosal bath (NaCl replaced with 120 mM Na gluconate). I_{sc} was measured at 1 data point every 10 s, with the convention that positive deflection represents the net movement of an anion in the serosal to mucosal direction. Transepithelial electrical resistance (TEER) was calculated according to Ohm's law, which is a summated value from both transcellular and paracellular resistances. The electrical impedance originating from the transcellular pathway represents the stability of the apical and basolateral plasma membranes, whereas the paracellular resistance is created when adequate cell-substrate or cell-cell contacts are formed in the RECs when cultured at an air-liquid interface. Amiloride (100 μM) (Spectrum chemical MFG corp, New Brunswick, NJ) was routinely added apically in order to abolish Na⁺ absorption. Forskolin (20 μM) (Sigma-Aldrich, St. Louis, Mo.) was then administered to both bathing solutions to stimulate cAMP-mediated Cl⁻ secretion. Cl⁻ secretory currents were identified on the basis of activation by forskolin and by sensitivity to the specific CFTR inhibitor INH-172 (10 μM) (Sigma-Aldrich, St. Louis, Mo.). Effect on the basolateral Na⁺/K⁺ ATPase pumps was evaluated in apical permeability studies utilizing 300 μM amphotericin B (Sigma-Aldrich, St. Louis, Mo.) applied to the apical membrane and ouabain (1 mM) (Sigma-Aldrich, St. Louis, Mo.) applied to the basal membrane. All drugs were added as a small volume of concentrated stock solution. Time-dependent reversibility studies were performed after washing the apical surface 3x with PBS following incubation. Blockade of TLR4 receptors was accomplished with TAK-242 (1 μM , Sigma-Aldrich, St. Louis, Mo.), while glutathione sulfhydryl reduced ethyl ester (GSH) (1 mM, Sigma-Aldrich, St. Louis, Mo.) was used to block ROS.

2.4. Patch clamp analysis

CFBE cells expressing WT CFTR cells on coverslips were transferred to an experimental chamber mounted on a microscope stage (Olympus). CFTR currents were recorded in whole-cell mode of the patch-clamp technique using an Axopatch 2000B amplifier interfaced with a computer through DIGITA 1440A, as previously described [47]. Recording pipettes were constructed from borosilicate glass capillaries (Warner Instruments, Hamden CT) using a Narishige PP83 microelectrode puller and fire-polished with a PP90 microforge (Narishige, Tokyo, Japan). Cells were perfused with an external solution of the following ionic composition (in mM): 145 CsCl, 2 MgCl₂, 2 CaCl₂, 5.5 Glucose, 10 HEPES pH 7.4 (1 N NaOH). The pipette resistance used for whole-cell recording ranged from 3 to 5 G Ω when filled with the following intrapipette solution (in mM): 135 CsCl, 10 KCl, 2 MgCl₂, 0.1 EGTA, 5.5 Glucose, 10 HEPES, pH 7.2 (1 N KOH). All experiments were performed at room temperature. Cells were continuously perfused with the external solution before and during the recording whole-cell configuration. The rate of perfusion was adjusted to 1 ml/min where the volume of the chamber was 0.5 ml, and the solution in the chamber was changed twice per minute. Conventional patch-clamp techniques were also adapted to record single-channel currents by cell-attached configuration. The pipettes were partially filled with a solution containing (in mmol/l) 135 CsCl, 10 KCl, 2 MgCl₂, 0.1 EGTA, 5.5 Glucose, 10 HEPES, pH 7.2 (1 N KOH) and had tip resistances of 6–8 M Ω . To obtain seals, bath solutions

contained (in mmol/l) 140 NaCl, 4.0 KCl, 1.8 CaCl₂, 1.0 MgCl₂, 10 glucose, 10 HEPES, pH 7.4. After seal formation, cells were perfused with potassium solution (150 mM) of the following composition: 150 mM KCl, 2 mM MgCl₂, 10 mM Hepes, pH 7.4 (1 N KOH), 5 mM Glucose. The osmolarity of the solution was adjusted to 300 milliosmoles using mannitol. This solution induces cell membrane potential depolarization to zero mV allowing easy control of the patch potential which will be $V_{\text{patch}} = -V_{\text{pipette}}$, since $V_{\text{m}} = 0 \text{ mV}$ [48–50]. Cells were incubated with LPS (10 $\mu\text{g/ml}$) for 4 h prior to patch formation. PBS vehicle controls were included in all studies. Single-channel recordings were analyzed using pClamp 10 software (AI). V_{com} = command potential. Tracings were filtered post-acquisition at 500 Hz. Current was normalized by the capacity of the membrane (pA/ μF).

2.5. Protein analysis

2.5.1. Western blotting

Cells were washed with ice-cold PBS 2x, then lysed with ice-cold RIPA buffer [50 mM Tris-HCl, 1% Nonidet P-40, 0.5% Sodium deoxycholate, 0.1% SDS, 150 mM NaCl, and Complete Protease Inhibitor (Roche Applied Science, Indianapolis, In.)]. Cell lysates were sonicated x3 for 10 s each, then spun for 30 min at 4 °C to collect the supernatant. Thirty μl of the supernatant was mixed with 4X Laemmli sample buffer +5% beta-mercaptoethanol and incubated at 37 °C for 30 min. Proteins were separated by SDS-PAGE (4–12% NuPAGE gels), transferred to polyvinylidene fluoride membranes (Bio-Rad, Hercules, CA, USA). CFTR was detected using MM13-4 mouse monoclonal antibody (N terminal 1:500, Sigma Aldrich, St. Louis, Mo. Catalog #: 05–581.) and anti-mouse IRDye labeled secondary antibodies and imaged using LI-COR system. TLR4 was detected with anti-TLR4 (Accession number O00206, 1:500, Novus Biologicals, Centennial, Co, Catalog# NB100-56579) and anti-rabbit IRDye labeled secondary antibodies and imaged using LI-COR system (Lincoln, Ne.). Densitometry [51] was performed with Image Studio Lite (Li-Cor, Lincoln, Ne.).

2.5.2. Biotinylation of surface CFTR

The expression of cell surface CFTR was measured after biotinylation using EZ-link® Biotin-LC-hydrazide (Thermo Fisher Scientific, Waltham, Ma.) [52]. CFBE cells were washed 3 times with pre-cold PBS then incubated with 5 mM Sodium Periodate which dissolved in PBS for 30 min at 4 °C. Then cells were washed 2 times with 100 mM Sodium Acetate (Ph 5.5) following by one PBS wash. 2 mM biotin-LC-hydrazide dissolved in Sodium Acetate solution was added to the cells for a 30 min incubation at 4 °C before cells were lysed in RIPA buffer. Cell lysates were spun down at 4 °C for 30 min and CFTR in the supernatant was then immunoprecipitated with 24-1 anti-CFTR C-terminal antibody (mouse monoclonal, Accession number P13569, Sanofi Genzyme, Cambridge, Ma. Hybridoma was purchased in 1998 and antibody produced/purified at the UAB hybridoma facility). Proteins were transferred to polyvinylidene fluoride membranes. Densitometry was performed with Image Studio Lite, (Li-Cor, Lincoln, NE, USA).

2.5.3. Measurement of carbonyl adducts in purified CFTR protein

WT CFBE cells with flag tagged WT CFTR grown on 10 cm Petri dishes at 90% confluence were treated with LPS (10 $\mu\text{g/ml}$), PBS, LPS + GSH (1 mM), or LPS + TAK242 (1 μM) for 4 h, then washed 3X with cold PBS and treated with lysis buffer (50 mM Tris HCl, pH 7.4, 150 mM NaCl, 1 mM EDTA, and 1% Triton X-100). For a reducing agent, 2-mercaptoethanol was added to the samples to attain a final concentration of 0.74 M. Cell lysis supernatants were collected and incubated with anti-flag M2 gel (Sigma-Aldrich, St. Louis, Mo. Catalog#: A2220) at 4 °C overnight under gentle rotation. Flag-tagged CFTR protein was eluted by 3X Flag Peptide (100 $\mu\text{g/ml}$, Sigma-Aldrich, St. Louis, Mo. Catalog# F4799) for 2 h at 4 °C according to the manufacturers protocol. The presence of protein carbonyl groups was assessed using the Oxyblot protein oxidation detection kit (Sigma-Aldrich, St. Louis, Mo. Catalog#

S7150), according to the manufacturer's protocol. Briefly, the carbonyl groups in the protein side chains were derivatized to 2,4-dinitrophenylhydrazone by reacting with 2,4-dinitrophenylhydrazine. Three μg of protein was used for each sample, and 2,4-dinitrophenol-derivatized protein samples were separated by polyacrylamide gel electrophoresis, as described previously [53]. Polyvinylidene fluoride membranes were incubated for 1 h in stock primary antibody (1:150 in 1% PBS/TBST buffer), and after washing, for 1 h in stock secondary antibody (1:300 in 1% PBS/TBST buffer). Membranes were washed $3 \times$ in TBST and visualized, as described previously [54,55]. The abundance of protein carbonylation was assessed by densitometry of each lane.

2.6. Reactive oxygen species

Measurement of ROS was performed as previously described [56]. For time-dependent studies, CFBE cells were seeded in 96-well plates at a density of 1×10^5 [5] and treated with 10 $\mu\text{g}/\text{ml}$ LPS up to 24 h. Time-dependent ROS production was measured from 15 min to 24 h according to the duration of LPS incubation. Cells were incubated with 25 μM carboxy-H2 dichlorohydrofluorescein (DCF) diacetate (Image-iT™ LIVE Green ROS Detection Kit, Thermo Fisher, Waltham, MA. Catalog# I-36007) for 30 min at 37 °C, then washed with warm HBSS 3 times and lysed with 100 μl Passive lysis buffer (Promega, Madison, WI. Catalog# E1941). ROS production was measured with cell lysis by fluorescence detection of Carboxy-DCF formation in a microplate reader excitation and emission filters centered at 485 and 525 nm. To evaluate ROS generation by confocal microscopy at the peak duration, CFBE cells were grown on glass-bottom petri dishes and treated with 10 $\mu\text{g}/\text{ml}$ LPS or PBS control for 4 h. After a gentle wash with warm Hank's buffered saline, cells were labeled with 25 μM carboxy-H2 DCF diacetate (Image-iT™ LIVE Green ROS Detection Kit, Thermo Fisher, Waltham, MA. Catalog# I-36007) for 30 min or incubated with 5 μM MitoSOX™ reagent (MitoSOX™ Red Mitochondrial Superoxide Indicator, Thermo Fisher, Waltham, MA. Catalog# M36008) for 10 min at 37 °C. Hoechst 33342 was added during the last 5 min for nuclear staining. Dyes were removed and cells were washed 3x before imaging 10x and 20x dry objectives in 1- μm steps at room temperature with a Nikon A1 confocal microscope and NIS-Elements Software (Nikon, Tokyo, Japan). Negative dye controls were obtained in cells without carboxy- H2 DCF diacetate or MitoSOX™ incubation. All images were processed at the same exposure time. The results were shown as the percentage of Carboxy-DCF or MitoSOX™ positive cells to total cell number using Image J (National Institutes of Health, Bethesda, MD).

2.7. Functional microanatomy

2.7.1. μOCT

ASL, periciliary liquid (PCL), CBF (ciliary beat frequency), and MCT can be measured simultaneously and non-invasively at the respiratory epithelial surface using μOCT , which generates cross-sectional images at 1- μm resolution through reflectance properties inherent to the airways [29,57–60]. The environment of the cells was controlled at all times during the experiments. A humidification chamber with conditions (37 °C, 5%CO₂) was used throughout the experiments. HSNE were evaluated after 4 h incubation of LPS (10 $\mu\text{g}/\text{ml}$) or PBS control. The imaging optics axis was placed within 10° of normal to the cell plane to reduce inaccuracies in geometric measurements [57]. Four regions of interest per each well were documented (2 points at 1 mm from the center and another at 1 mm from the edge for 2 different locations) and averaged for a single value per well. ASL and PCL were calculated by direct measurement of the visible depth within the image. To account for refractory properties of the liquid, layer thickness measurements were corrected for the refraction index of the liquid ($n = 1.33$). ASL and PCL depth were calculated from pixels to μm using a ratio of 0.82. CBF was evaluated by means of a time series of images by ascertaining peak amplitude frequency in the temporal Fourier transform of areas

demonstrating oscillatory behavior [61]. Measurements were performed at 5 uniformly distributed locations for each region of interest and then averaged. Statistics were performed for each individual well replicate. All images were analyzed using ImageJ version 1.50i (National Institutes of Health, Bethesda, MD) and MATLAB® R2016a (The MathWorks, Natick, MA).

2.7.2. Confocal laser scanning microscopy of ASL fluorescent indicator

ASL was also measured using confocal laser scanning microscopy to confirm LPS-induced depletion. Murine REC filters were washed 3 times with PBS the day before the experiment. Cells were incubated with apically applied LPS (10 $\mu\text{g}/\text{ml}$) or PBS control solution (10 μl volume) for 4 h 100 μM CellTracker™ Green BODIPY® (Invitrogen, Carlsbad, CA. Catalog# C2102) was administered to the basolateral medium 3 h before imaging and 20 μl 10 mg/ml Texas Red® (Invitrogen, Carlsbad, CA. Catalog# D-1863) in FC-70 (Fluorinert FC-70, Thermo Fisher, Waltham, MA. Catalog# NC 9062226) to the apical side 30 min before imaging [62]. Imaging was performed with a Zeiss LSM 710 Confocal Microscope using Zeiss Plan Apo 20x .8 na dry objective in 1- μm steps at room temperature. Values for each monolayer were derived from three regions of interest. ASL depth was measured in the orthogonal (head on X-Z) image view [48,49].

2.8. Nasal potential difference assay

LPS (10 $\mu\text{g}/\text{ml}$) +/- GSH (1 mM, Sigma-Aldrich, St. Louis, Mo.) or TAK242 (1 μM , Thermo Fisher, Waltham, MA.), and PBS vehicle control solution was mixed in a thermal transition gel (PureRegen gel, Jacksonville, Fla.) and instilled intranasally in C57BL/6 mice for 4 h ($n = 6$ per condition). A modified three-step protocol was used, as described previously [63–65]. First, nasal cavities of anesthetized C57/BL/6 mice were perfused with Ringer's solution containing 148 mM NaCl, 4 mM KCl, 1.2 mM MgCl₂, 2.25 mM CaCl₂, 2.4 mM K₂HPO₄, 0.4 mM KH₂PO₄ (pH 7.4). Second, an identical solution with amiloride 100 μM to inhibit Na⁺ absorptive pathways was perfused. Finally, a zero-Cl⁻-containing solution (NaCl in solution #1 replaced by 148 mM Na gluconate, 2.25 mM Ca gluconate, and 4 mM K gluconate; pH 7.4) was perfused + forskolin 20 μM to gauge Cl⁻ secretion across the nasal epithelium. The activity was measured from the stable baseline to the highest point of hyperpolarization. All traces were interpreted in a blinded fashion.

2.9. Lactate dehydrogenase (LDH) assay

Cellular toxicity was evaluated as previously described [25,66]. Relative cell viability in the presence of LPS reflects concentrations of released LDH enzyme originating from damaged MNSEs. Released LDH at 4 h after incubation was measured with a coupled enzymatic reaction that converted a tetrazolium salt (iodonitrotetrazolium) into the red color formazan (Sigma-Aldrich, St. Louis, Mo. Catalog# Tox-7). Quantification of LDH was determined from the concentration of the converted formazan within the 20 min of incubation. The resulting formazan absorbs maximally at 492 nm and can be measured quantitatively at 490 nm. Total LDH in each sample was expressed in nanograms per milliliter (ng/mL).

2.10. CFTR gene expression

Total RNA was isolated from 4-h LPS or PBS control-treated filters with RNeasy mini kit (Qiagen, Valencia, Ca) according to the manufacturer's instructions [67]. To prevent possible DNA contamination, samples were pretreated with RNase-free DNase (Qiagen) and column purified. Sequences used for murine CFTR and 18S rRNA were purchased from Assays on Demand (Thermo Fisher, Waltham, MA.) with assay ID for murine CFTR, Mm00445197_m1. A one-step PCR protocol was used to quantify CFTR mRNA transcripts by an Prism 7500 sequence detection system according to the manufacturer's instructions. TaqMan

OneStep PCR Master Mix Reagents Kit was used for reverse transcription and PCR. All experiments were performed in triplicates.

2.11. cAMP ELISA

Cellular cAMP was measured using an ELISA-based detection kit (Cayman Chemicals, Ann Arbor, MI) as previously described [68,69]. MNSEs were incubated with LPS or PBS control for 4 h on the apical side. Forskolin (20 μ M)-stimulated cAMP levels were also measured after 15min incubation. Apical fluid was removed, and cells were washed 3 times with ice-cold PBS. Ice-cold ethanol was used to extract cellular cAMP. The supernatants were vacuum dried, and the cAMP levels were quantified per the manufacturer's directions.

2.12. Statistical analysis

Descriptive statistics were computed and numbers compared using Student's *t*-test (two-sided) or analysis of variance followed by Tukey-Kramer multiple comparison test as appropriate. All tests were performed using GraphPad Prism (GraphPad Software, Inc., La Jolla, CA). All error bars designate standard deviation, with significance set at $p \leq 0.05$.

3. Results

3.1. LPS decreases CFTR-dependent ion transport in mammalian REC

Using exposures to physiologically relevant concentrations based on

GNB infection *in vivo*, [70–74] LPS derived from *P. aeruginosa* (Sigma Aldrich, St. Louis, Mo.) was administered to the apical surfaces of primary MNSE cultures in dose and time-dependent fashion to test the effects of early exposure on forskolin-stimulated transepithelial Cl^- transport. A single incubation with LPS added to the apical membrane caused a significant and dose-dependent reduction in CFTR-dependent ion transport (Fig. 1A–C) with peak effects at 4 h and a concentration of 10 $\mu\text{g}/\text{ml}$ (used for all subsequent studies). There was a significant decrease in amiloride-sensitive Isc (in $\mu\text{A}/\text{cm}^2$) (LPS, 2.8 ± 0.8 vs. Control, 3.5 ± 1.1 , $p \leq 0.05$, $n \geq 20$) which was consistent with previous investigations [75]. Forskolin-stimulated Isc (LPS, 20.6 ± 3.2 vs. Control, 26.7 ± 2.5 , $p \leq 0.001$, $n \geq 20$) and inhibition with CFTRinh-172 (LPS, 16.0 ± 4.3 vs. Control, 19.9 ± 6.5 , $p \leq 0.05$, $n \geq 20$) were both significantly reduced, indicating an LPS-induced acquired deficiency in CFTR-mediated Cl^- secretion (Fig. 1D). The impact of LPS exposure was conserved across the tested mammalian REC's including CFBE-WT cells (LPS, 112.1 ± 18.2 vs. Control, 133.5 ± 20.9 , $p \leq 0.01$, $n = 13$), HSNE (LPS, 32.2 ± 4.1 vs. Control, 38.3 ± 6.2 , $p \leq 0.01$, $n = 12$), and rabbit nasal epithelial cells (LPS, 29.3 ± 7.6 vs. Control, 35.9 ± 5.4 , $p \leq 0.01$, $n \geq 12$) (Fig. 1E) in primary culture. Co-incubation with the TLR4 inhibitor TAK242 eliminated the effect of LPS on Isc in MNSE confirming CFTR-mediated Cl^- secretion reduction is dependent on activity of this pattern recognition receptor (LPS, 11.5 ± 2.1 vs. LPS + TAK-242, 15.0 ± 2.2 , $p \leq 0.05$, $n \geq 6$) (Fig. 1F). A small but significant effect on the basolateral $\text{Na}/\text{K} + \text{ATPase}$ was noted with apical permeabilization and ouabain treatment (Supplementary Figure 1), indicating that LPS added to the apical membrane also inhibited the basolateral $\text{Na}^+/\text{K}^+ \text{ATPase}$. LPS also did not induce cellular toxicity since there was no increase in

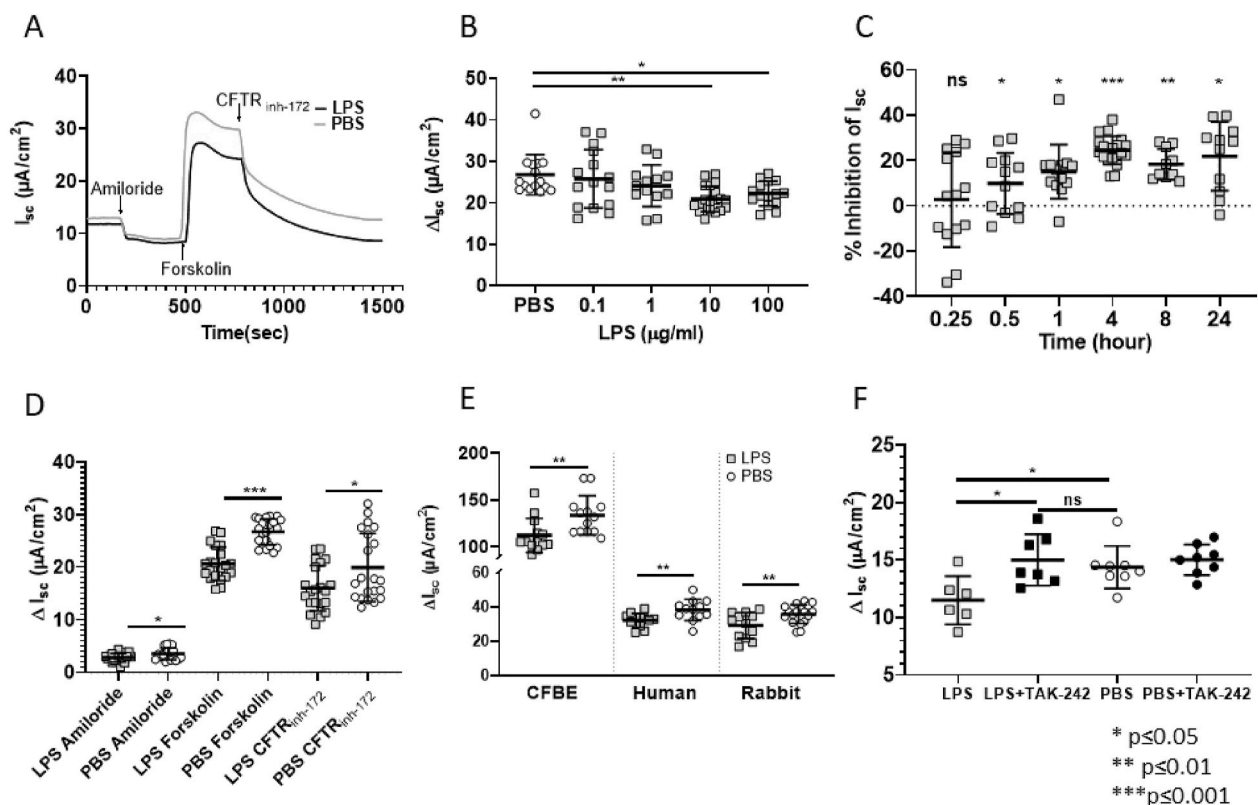


Fig. 1. (A–D) LPS incubation in MNSE induces acquired CFTR dysfunction. (A) Representative Ussing chamber current tracings of MNSE treated with LPS (10 $\mu\text{g}/\text{ml}$) or PBS control for 4 h. Sequential addition of amiloride (100 μM), forskolin (20 μM), and CFTRinh-172 (10 μM) are shown. (B) Change in forskolin-dependent I_{sc} of MNSE treated with increasing concentrations of LPS or vehicle control for 4 h reveals decreased Cl^- secretion with a plateau at 10 $\mu\text{g}/\text{ml}$, $n \geq 13$. (C) Time-dependent changes in forskolin-induced ΔI_{sc} following incubation of LPS (10 $\mu\text{g}/\text{ml}$) demonstrates decreased Cl^- secretion with longer incubation and a plateau at 4 h, $n \geq 10$. (D) Summary of I_{sc} measurements at optimal time (4 h) and dosing (10 $\mu\text{g}/\text{ml}$). All values are significantly different from each other (amiloride, $p \leq 0.05$; forskolin, $p \leq 0.001$; CFTRinh-172, $p \leq 0.05$, $n \geq 20$). (E) LPS-induced acquired CFTR dysfunction was consistent across mammalian RECs. CFBE-WT, human sinonasal epithelial cells, and rabbit nasal septal epithelial cells were all significantly decreased compared to PBS vehicle control by approximately 20% of CFTR-mediated I_{sc} ($p \leq 0.01$, $n \geq 12$). (F) Co-incubation with the TLR4 inhibitor TAK242 (1 μM) eliminated LPS-dependent inhibition of CFTR-mediated I_{sc}.

LDH release or reduced TEER at this dose and concentration (Supplementary Fig. 2A and 2B) and normal levels of forskolin-stimulated I_{sc} were restored by 3 h following removal of LPS (Supplementary Figure 3).

3.2. LPS abrogates CFTR currents by reducing open channel probability

CFBE-WT cells were subjected to whole-cell patch-clamp analysis to characterize impact of LPS on CFTR function at the cellular level (Fig. 2). LPS incubation resulted in near-complete inhibition of forskolin-induced currents (in pA/pF) (LPS + Forskolin, 0.34 ± 0.11 vs. Control + Forskolin, 79.06 ± 21.7 , $p \leq 0.001$, $n = 9$). Similar to Ussing chamber experiments, co-incubation with the TLR4 inhibitor TAK-242 eliminated the effect of LPS, indicating that activation of TLR4-mediated pathways is necessary for this response (+Tak-242, 92.57 ± 13.1 , $p \leq 0.001$, $n = 9$). We observed more substantial inward (nearly complete) than outward ($\sim 50\%$ at -100 mV) current inhibition. Single-channel patch-clamp analysis was performed in cell-attached mode with a holding potential of -100 mV (Fig. 3). Single-channel conductances were approximately 6.5 pS with a single event amplitude of 6.5 pA consistent with what was previously reported for CFTR [47,69]. The activity was measured after cells were incubated with or without LPS following the addition of $10 \mu\text{M}$ forskolin and $100 \mu\text{M}$ IBMX. While unitary conductances and single-channel amplitudes were unaffected by LPS, the number of active channels and their open probability (NPo) in the membrane were markedly decreased (LPS, 0.4 ± 0.1 vs. Control, 1.5 ± 1.2 , $p \leq 0.01$, $n = 10$). Taken together with the whole-cell recordings indicating uneven rectification, the decrease in channel open probability confirms that LPS treatment leads to changes in CFTR function.

3.3. Total and cell surface CFTR levels are unaffected by LPS exposure

Western blot analysis in MNSE (using the rat monoclonal anti-CFTR antibody, 3G11) and CFBE-WT (mouse monoclonal anti-CFTR antibody, MM13-4) revealed no changes in total CFTR levels (MNSE, LPS 1.16 ± 0.18 vs. control, 1.0 ± 0.34 , $n = 5$ and CFBE-WT, LPS 1.07 ± 0.08 vs. 1.0 ± 0.05 , $n = 6$) (Fig. 4A and B). TLR4 protein levels were also unaffected by LPS incubation (CFBE-WT, 1.03 ± 0.10 vs. 1.0 ± 0.07 , $n = 6$). CFBE cells were used to measure surface CFTR and TLR4 due to greater protein expression and availability of antibodies for both immunoprecipitation and Western blot. CFTR has been reported previously to extract and endocytose LPS [36]. Since total CFTR levels did not change, we wanted to test if there was change in the distribution of CFTR following LPS treatment. To evaluate whether reduced I_{sc} resulted from diminished cell surface CFTR (sCFTR), cell surface proteins were biotinylated [52]. Following lysis, total CFTR was immunoprecipitated (mouse monoclonal anti-CFTR C-terminal antibody, 24-1), subjected to SDS-PAGE and Western blot. Biotinylated CFTR was detected with SA-HRP. No significant changes in cell surface CFTR levels were observed (Fig. 4C). To test the sensitivity of the cell surface biotinylation assay to detect surface CFTR, we applied cAMP to enhance surface CFTR levels [52]. Consistent with previous findings, we measured 10–15% increase in sCFTR levels in response to forskolin ($20 \mu\text{M}$) in both LPS (LPS, 1.06 ± 0.10 vs. +cAMP 1.33 ± 0.03 , $p \leq 0.001$, $n = 6$) and control samples (PBS, 1.0 ± 0.06 vs. +cAMP 1.25 ± 0.04 , $p \leq 0.001$, $n = 6$).

These results confirm that reduced transepithelial currents (I_{sc}) at this dose and incubation are not the result of decreased CFTR protein expression at the apical surface. Furthermore, CFTR mRNA levels at 4-h LPS incubation were not significantly different (Supplementary Figure 4).

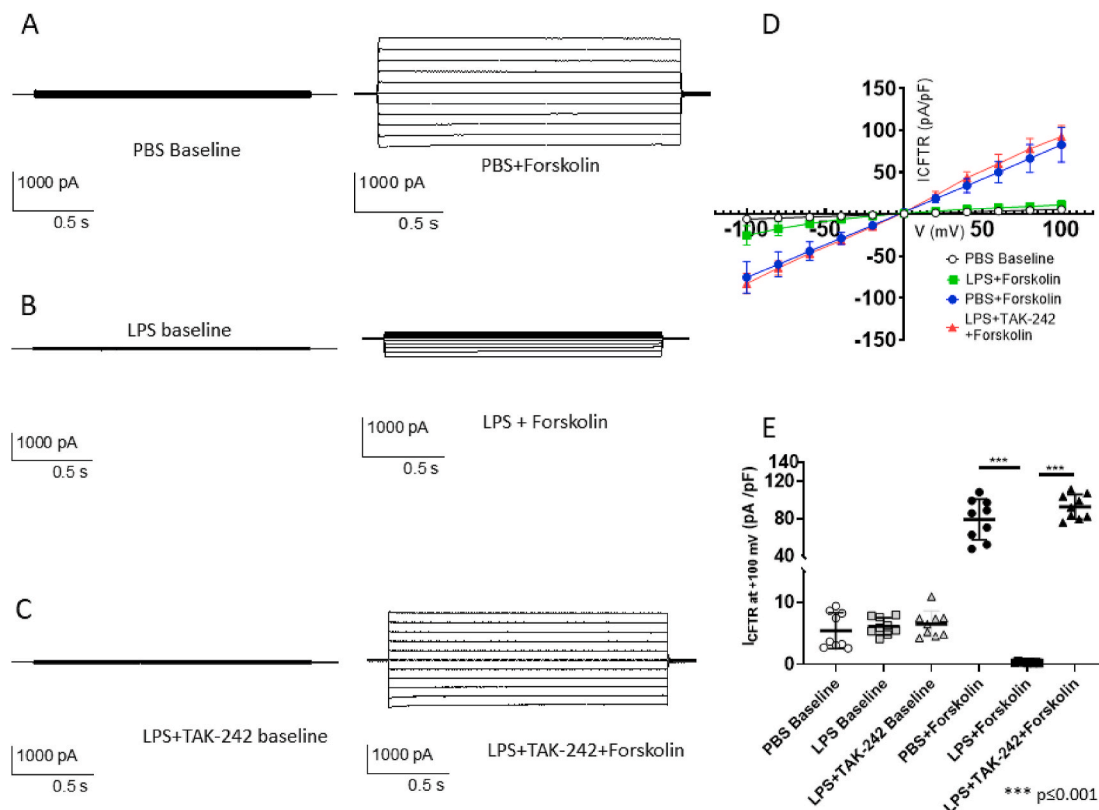


Fig. 2. (A–C) Whole-cell patch-clamp recording from CFBE-WT cells exposed to PBS, LPS ($10 \mu\text{g/ml}$), or LPS + TAK-242 ($1 \mu\text{M}$). (D) IV curves for the same conditions normalized to the capacity of the membrane (in pA/pF). LPS nearly completely inhibited activation of Cl^- current. (E) Summary of currents at 100 mV for cells co-incubated with PBS, LPS, and TAK-242. Cl^- current activated by forskolin in LPS + TAK-242 group was significantly increased ($p \leq 0.001$, $n = 9$) and similar to PBS vehicle control + forskolin.

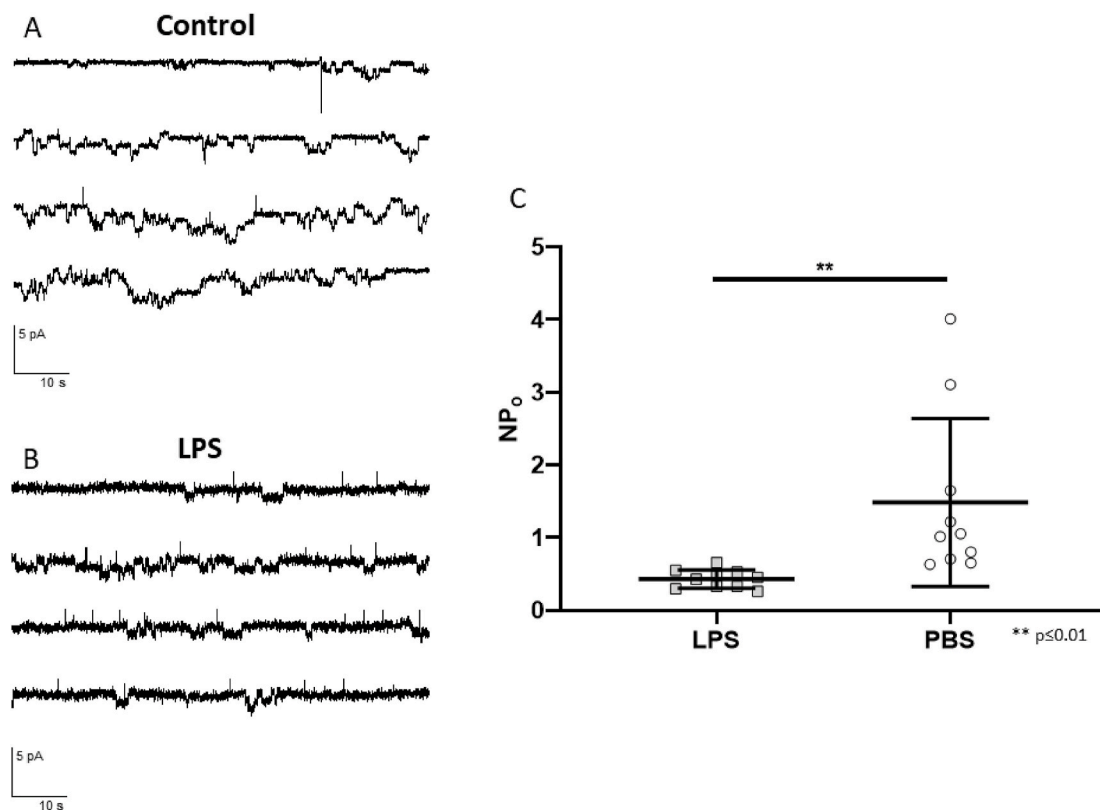


Fig. 3. (A&B) Single channel patch-clamp with 4-h LPS (10 $\mu\text{g}/\text{ml}$) incubated CFBE-WT cells shows the CFTR open probability and number of active channels were markedly decreased. (C) LPS significantly reduced the number of active channels and their open probability shown here as NP_o ($p \leq 0.01$, $n = 10$).

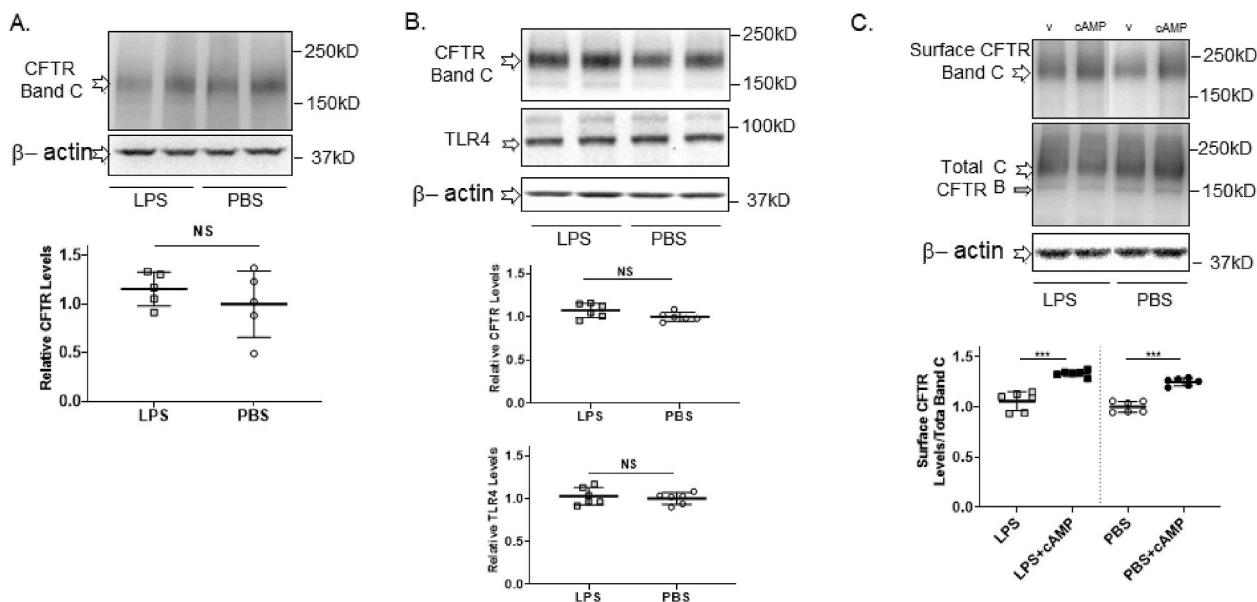


Fig. 4. LPS treatment does not alter CFTR levels. (A) CFTR Western blot from MNSE. MNSE were grown on permeable supports, tested in Ussing chambers, followed by lysis and assessment of CFTR protein levels by WB. Biological duplicates of LPS (10 $\mu\text{g}/\text{ml}$) and PBS-treated samples are shown on top. CFTR levels are plotted relative to beta-actin; $n = 5$, $p > 0.05$ (NS). (B) CFTR and TLR4 Western blot from CFBE cells. CFBE cells were treated with LPS or PBS. Western blots of biological duplicates of CFTR and TLR4 with beta-actin as loading control are shown on top. CFTR and TLR4 levels were plotted relative to beta actin. $n = 6$. (C) Cell surface and total CFTR levels in CFBE cells following cAMP (10 min forskolin 20 μM), LPS and LPS + cAMP treatment. cAMP enhances cell surface CFTR levels equally in LPS and PBS-treated cells ($p \leq 0.001$, $n = 6$). Surface CFTR levels are shown on top v = vehicle, cAMP = cAMP treatment. Following biotinylation, only Band C CFTR was pulled down (top). Total CFTR levels are shown in the middle. Both band B and C are present. Beta actin was used as loading control for total CFTR. Surface CFTR levels were plotted relative to total CFTR Band C levels; ***: $p \leq 0.001$.

3.4. Evidence for the contribution of LPS-induced ROS to CFTR dysfunction

LPS-induced intracellular ROS accumulation in CFBE cells (as measured by the oxidation of 20,70-DCF diacetate to fluorescent DCF) occurs in a time-dependent fashion with a single exposure at a peak effect of 4 h similar to reductions in *I*_{sc} noted in the Ussing chamber (Supplementary Figure 5). Cytoplasmic and mitochondrial ROS (percentage of fluorescent cells) were significantly elevated after 4 h of LPS exposure (cytoplasmic, LPS, 38.44±/−4.61% vs. PBS control, 15.37 ± 3.27%, *p*≤0.001, *n* = 11 and mitochondrial, LPS, 55.64 ± 15.14% vs. PBS control, 36.64 ± 12.47%, *p*≤0.01, *n* = 12) as visualized with confocal microscopy (Fig. 5). Further, co-incubation of cells with LPS and the ROS scavenger, glutathione (GSH), eliminated the impact of LPS exposure on CFTR in the Ussing chamber (in μAmp/cm²) (Fig. 6A, LPS, 23.94 ± 2.88 vs. +GSH, 31.17 ± 2.83, *p*≤0.001, *n*≥6) and whole-cell patch-clamp analysis (in pA/pF) (Fig. 6B, LPS, 9.67 ± 1.09 vs. +GSH, 50.18 ± 4.77, *p*≤0.001, *n* = 10). Carbonylation of CFTR (a consequence of oxidation) was significantly increased with LPS exposure (LPS, 32.21 ± 21.50 vs. PBS control, 1.00 ± 0.81, *p*≤0.01, *n* = 5) and levels were comparable to control when incubated with GSH (6.50 ± 5.44) or the TLR4 inhibitor TAK-242 (5.50 ± 6.13) (Fig. 6C&D). Carbonylation of band B was not observed. Immature band B resides in the endoplasmic reticulum and may not have susceptible arginine, proline, lysine, or threonine residues, which would be prone to carbonylation during exposure to LPS. In comparison, band C has passed through the Golgi apparatus and is fully mature and thus may have susceptible amino acids on the periphery exposed to carbonylation. The absence of reduced adenyl cyclase-mediated cAMP production with LPS exposure indicates that ROS impacts CFTR directly rather than through PKA-mediated pathways (Supplementary Figure 6). These results strongly support the hypothesis that LPS-induced ROS production contributes to reduced

CFTR function.

3.5. MCT and other markers of airway functional microanatomy are decreased following LPS exposure

It is established that inhibition of transepithelial Cl[−] secretion leads to airway surface dehydration and diminished ASL and PCL depth, as well as consequent effects on the mucociliary transport apparatus, such as CBF [46,76,77]. In HSNE cultures, μOCT was used to assess changes to markers of mucociliary function after LPS incubation with or without GSH or TAK-242 (Fig. 7). Mean ASL and PCL depth thickness (μm) were significantly reduced in the LPS group when compared to the control group and when administered with GSH or TAK-242 (ASL; LPS, 4.28 ± 0.53 vs. PBS, 8.06 ± 1.56; LPS + GSH, 8.65 ± 1.63; LPS + TAK-242, 8.27 ± 1.63; *p*≤0.001, *n*≥9; PCL; LPS, 2.98 ± 0.46 vs. PBS, 4.74 ± 0.58; LPS + GSH, 4.48 ± 0.38; LPS + TAK-242, 4.76 ± 0.31; *p*≤0.001, *n*≥9). Mean CBF (Hz) was also significantly reduced with exposure to LPS compared to controls and addition of GSH and TAK-242 (LPS, 7.70 ± 1.22 vs. PBS, 9.15 ± 1.21; LPS + GSH, 9.01 ± 0.81; and LPS + TAK-242, 9.05 ± 0.89; *p*≤0.05, *n*≥9). MCT was markedly inhibited in the LPS group when compared PBS control vehicle (0.14 ± 0.07 mm/min vs. 0.45 ± 0.33 mm/min, *p*≤0.001, *n* = 12) and when co-incubated with GSH and TAK-242 (0.36 ± 0.06 mm/min and 0.36 ± 0.04 mm/min; respectively; *p*≤0.05, *n*≥9). In MNSE cells, ASL depth was significantly reduced according to confocal microscopy z-stacked images; thus replicating our findings (with identical conditions) using another established technique. (Red-ASL; Green-Cell marker; 3.93 ± 0.32 vs. Control 5.19 ± 0.59, *p*≤0.001, *n*≥11).

3.6. LPS inhibits nasal potential difference in vivo

Given our *in vitro* findings of acquired CFTR dysfunction in MNSE, we

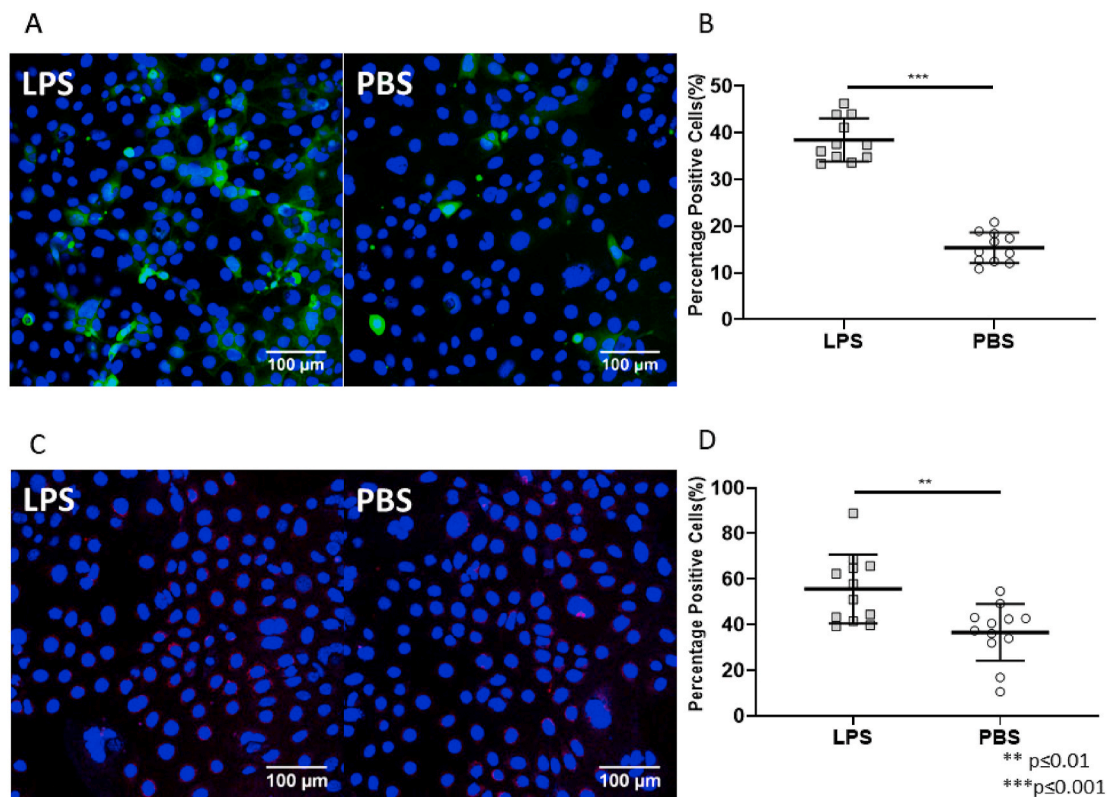


Fig. 5. (A & B) Cytoplasmic (green) and mitochondrial (red) ROS were significantly increased after LPS (10 μg/ml) exposure in CFBE cells. (C) The percentage of positive cells in LPS group was 2.5x higher (*p*≤0.001, *n* = 11) than the control for cytoplasmic ROS and (D) 1.52x higher (*p*≤0.01, *n* = 12) for mitochondrial ROS. (***p*≤0.01, ****p*≤0.001). (For interpretation of the references to color in this figure legend, the reader is referred to the Web version of this article.)

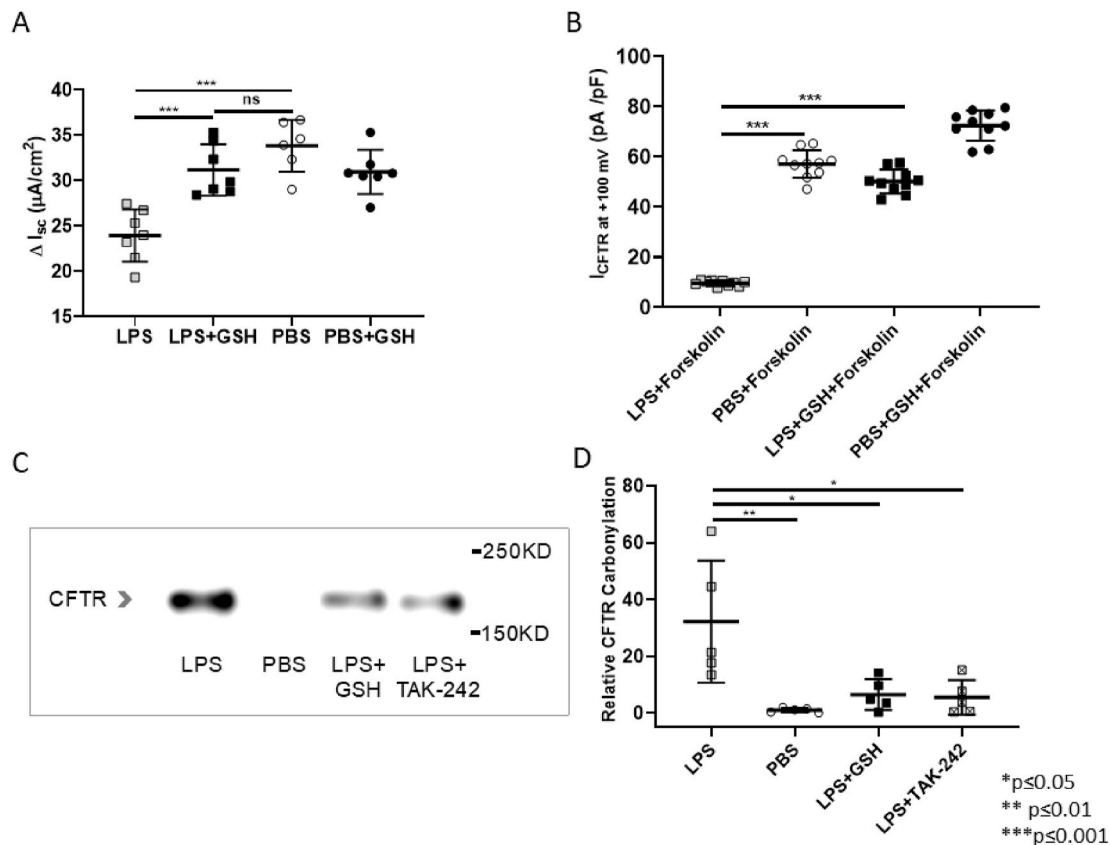


Fig. 6. CFTR dysfunction was eliminated with the ROS scavenger GSH (1 mM). LPS + GSH co-incubation significantly increased Cl⁻ transport compared to LPS only levels ($p \leq 0.001$) in both Ussing chamber (A) and whole-cell patch-clamp (B) to a level comparable to PBS controls (C&D). CFTR protein carbonylation was increased after exposure to LPS, and normalized with LPS + GSH or LPS + TAK-242 (1 μ M) co-incubation to levels similar to vehicle. (* $p \leq 0.05$, ** $p \leq 0.01$, *** $p \leq 0.001$, ns = no significance).

next tested LPS exposure in C57BL/6 mice *in vivo* (Fig. 8). LPS (10 μ g/ml) +/- GSH (1 mM) or TAK-242 (1 μ M) or PBS control solution embedded in a thermal transition gel were instilled intranasally for 4 h. LPS significantly reduced Cl⁻ secretion across the nasal epithelium measured by NPD assay in response to low Cl⁻ forskolin solution by approximately 30% (in mV; LPS, 4.98 ± 1.46 vs. Control, 7.34 ± 1.59 , $p \leq 0.05$, $n = 6$). When co-incubated with GSH or TAK-242, the response to low Cl⁻ forskolin was similar to control vehicle and significantly improved over LPS incubation alone (GSH, 7.84 ± 1.40 and 7.36 ± 1.20 , $p \leq 0.05$, $n = 6$). This confirmed the findings that were observed *in vitro* were reflective of the *in vivo* situation following LPS exposure.

4. Discussion

This study demonstrates that brief exposures to physiologically relevant concentrations of LPS lead to a localized, CF-like mucosal dysfunction in mammalian RECs. LPS inhibited cyclic AMP-activated CFTR Cl⁻ currents by decreasing the number of active channels and their open probability. The decrease in channel activity may be the result of channel deactivation (due to post-translational modification or alteration of signal transduction) and/or removal of channels from apical membranes. Our biotinylation studies show that CFTR Band C levels remain unchanged after LPS treatment (Fig. 4C). This led us to propose that the LPS-induced decrease of active CFTR channels was caused by deactivation of CFTR channels in the apical membrane. In Ussing chambers, CFTR-mediated Cl⁻ secretion was significantly reduced as early as 30 min following LPS exposure with peak effects at 4 h and 10 μ g/ml concentration without inducing cell death or deleterious effect on TEER. Although almost complete inhibition of forskolin-stimulated Cl⁻ secretion measured in cells isolated with patch clamp was

observed, there was a smaller, 20% reduction in forskolin-stimulated current change in the Ussing chamber after LPS exposure occurred. In contrast to patch clamping studies, vectorial transport of Cl⁻ ions across confluent monolayers depends on a number of transporters (such as the Na-K-ATPase, Na-K-Cl cotransporter, K channels etc.). In addition, human sinonasal epithelial cell cultures contain small percentages of other cells that may influence the results. Regardless, the degree of CFTR functional inhibition by LPS was sufficient to reduce epithelial function including ASL, PCL, CBF, and MCT. The severity of the ion transport and functional microanatomy abnormalities were intermediate compared with the congenital absence of CFTR (no Cl⁻ transport) observed in CF epithelial cells, but were capable of producing pronounced defects in mucociliary function at levels that would elicit poor mucociliary clearance and mucus retention *in vivo* especially if the exposure is persistent [78]. Importantly, the *in vitro* results were confirmed following *in vivo* exposure of mice to LPS that led to a marked decrease in transepithelial Cl⁻ transport across the murine nasal airway with 4-h incubation.

Our results indicate that LPS exposure resulted in elevated cytoplasmic and mitochondrial ROS levels and CFTR carbonylation, a post-translational modification that may also lead to reduced CFTR protein stability, reduced function and thickened airway secretions [20,79–82]. Indeed, the production of ROS induced by nitric oxide in LLC-PK1-cells stably expressing CFTR, as well as in human airway epithelial cell monolayers, decreased wild type CFTR levels and was accompanied by CFTR nitration [83]. These changes in CFTR levels and posttranslational nitration were accompanied by reduced cAMP-activated Cl⁻ currents [16]. Although these studies applied a more prolonged (24–48 h) exposure to nitric oxide, it is possible that the produced ROS and CFTR carbonylation following LPS treatment can also lead to reduced CFTR levels after a long exposure, but was not studied in the current project.

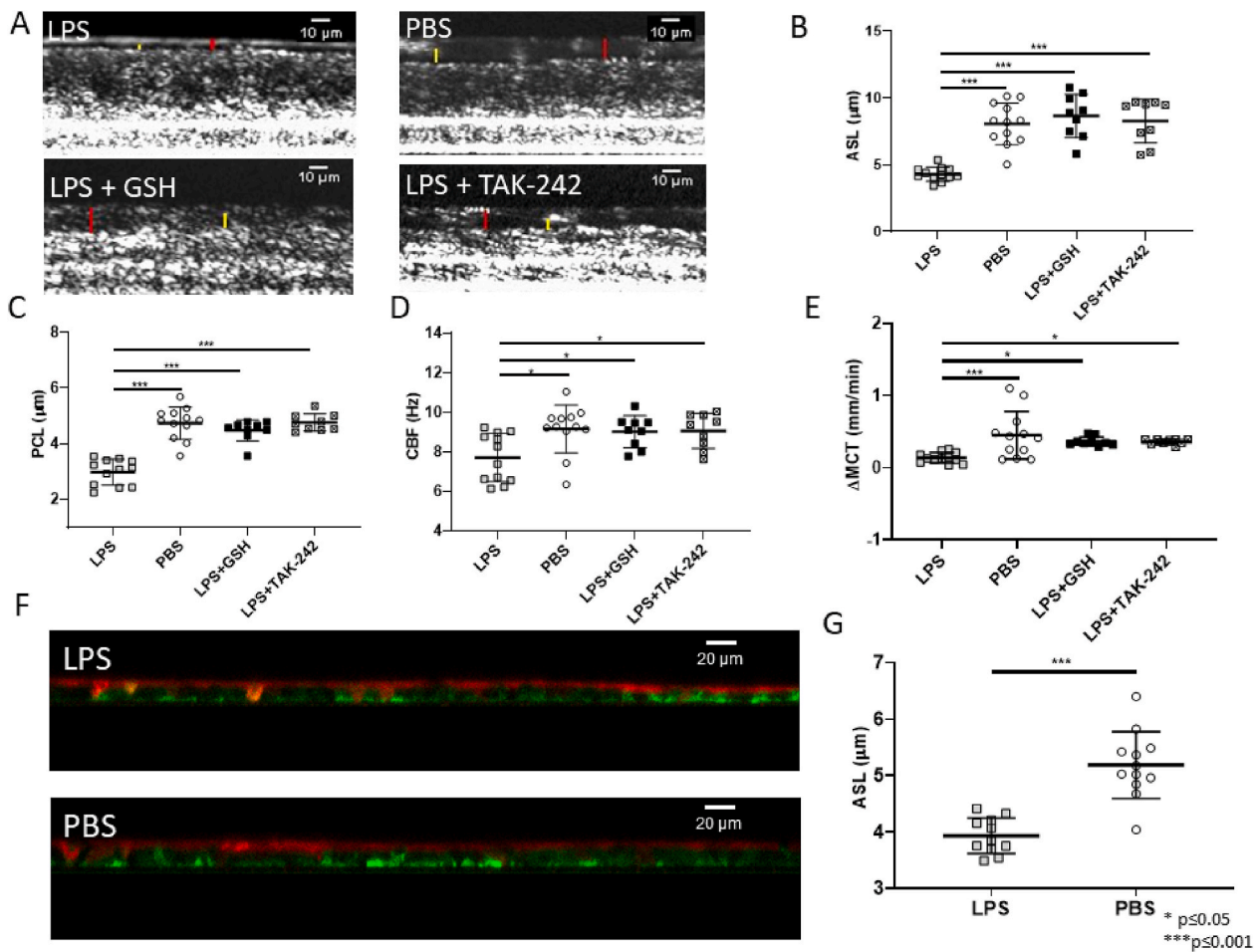


Fig. 7. μ OCT of HSNE shows airway surface liquid, periciliary liquid, ciliary beat frequency, and mucociliary transport were all significantly reduced after LPS (10 μ g/ml) incubation - an effect that was eliminated with co-incubation with GSH (1 mM) and TAK-242 (1 μ M). A: Cross sectional μ OCT images of HSNE treated with LPS (10 μ g/ml) +/- GSH (1 mM) or TAK-242 (1 μ M) or PBS vehicle control for 4 h. ASL depth (red bar) and PCL depth (yellow bar) are demarcated. B-E: Summary data showing ASL depth (B), PCL depth (C), CBF (D), and MCT (E). F: In MNSE, cells were stained to visualize overlying surface liquid. Confocal images demonstrate decreased ASL depth from inhibition of apical Cl^- secretion (red-ASL; green-cell marker). G: LPS significantly decreased ASL depth (in μ m) in murine nasal septal epithelial cultures (* $p \leq 0.05$, *** $p \leq 0.001$). (For interpretation of the references to color in this figure legend, the reader is referred to the Web version of this article.)

These observations suggest that during a chronic infection multiple pathways may contribute to reduced CFTR function and acquired CF-like symptoms.

Our evidence for functional changes to CFTR implicate early oxidative stress as the primary mechanism responsible for LPS-induced acquired CFTR dysfunction based upon: 1) decreased open probability of CFTR, 2) reduced number of active channels without a concomitant decrease in surface levels of CFTR, 3) elimination of cAMP/PKA dependent effects as a source of the reduction, and 4) co-incubation with GSH eliminating the impact on CFTR function, MCT, and carbonylation. While there was a significant decrease in amiloride-sensitive I_{sc} , this was consistent with previous observations by Boncoeur and colleagues [75] who found that LPS decreased αENaC in alveolar epithelial cells by $\sim 50\%$ in as little as 4 h by induction of ROS. Changes here could be attributable in part to a small, but significant effect on basolateral Na/K + ATPase pumps noted with apical permeabilization as seen in [Supplementary Figure 1](#). This could decrease the driving force for apical cation and anion transport. However, this does not appear to be the primary mechanism of reduced cAMP-stimulated currents and cannot explain the impact on CFTR open probability. Reactive species generated intracellularly may oxidize cysteines and cause a number of additional post translational modifications which may result in loss of CFTR function. CFTR possesses 18 cysteine residues that are potential targets, and several oxidized forms of GSH have been shown to glutathionylate

and inhibit the CFTR channel [84]. The identification of carbonyl adducts only represents a correlation and not a causal relationship. To prove this, identification of specific residues modified by LPS-generated ROS require mass spectrometry studies of purified CFTR. The very small quantities of CFTR in apical membranes of respiratory epithelial cells stymied our attempts to conduct these studies. Determining the biogenetic and structural modifications that confer loss of function to CFTR protein will offer vital insight regarding critical areas of inhibition, and describe a new method utilized by human pathogens such as *Pseudomonas* to abrogate the normal MCT mechanism. Such information is crucial for identifying new therapeutic targets for both CF and non-CF airway disease.

Conditioned media of PAO1 strain of *P. aeruginosa* has also been shown to trigger changes to respiratory epithelial function, primarily through endoplasmic reticulum stress and subsequent activation of the unfolded protein response (UPR) [85]. While the authors attributed the effects to pyocyanin and other secreted factors, LPS was not evaluated. Importantly, UPR activation leads to inhibition of CFTR transcription as well as reduction in CFTR maturation [86,87]. Given the early functional response to LPS in our studies and the lack of change in total and surface CFTR protein, or mRNA levels, it is unlikely that oxidative stress or activation cellular stress responses such as UPR or the integrated stress response (ISR)-mediated CFTR expression reduction was involved in the functional changes. In other words, the markedly reduced CFTR

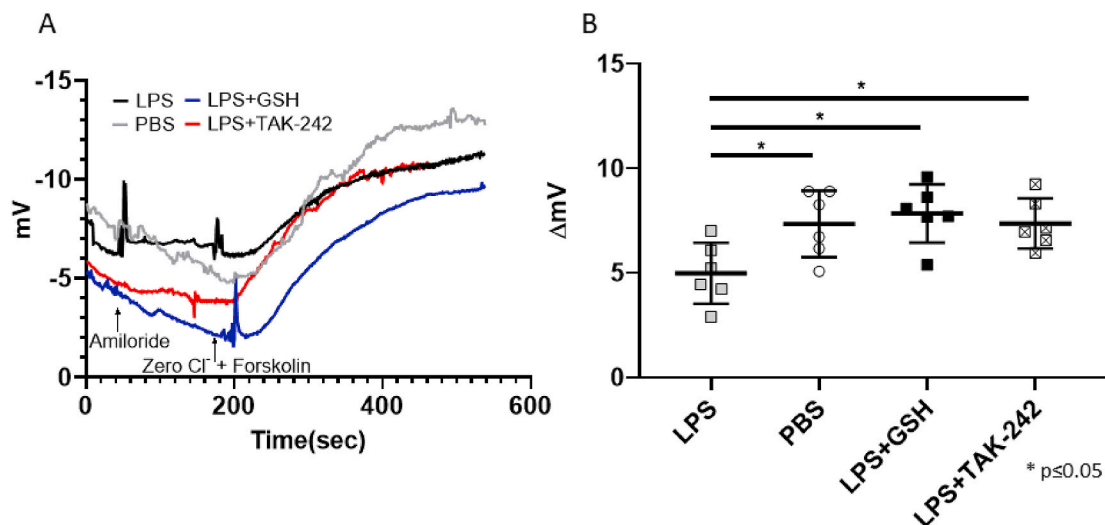


Fig. 8. Mouse NPD tracings after 4-h exposure to LPS (10 μ M) +/- GSH(1 mM), or LPS + TAK242(1 μ M), LPS, and PBS control vehicle were loaded in a thermal-based transition gel injected into the mouse nasal cavity. (A) Catheter is inserted into the nostril for perfusing solutions and a skin bridge placed subcutaneously in the lower back. (B) Tracing represents the sequential administration of Ringer's solution, Ringer's solution + amiloride, and zero Cl⁻ + amiloride + forskolin. (C) Summary of nasal potential difference measurements due to zero Cl⁻ + forskolin administration. Transepithelial Cl⁻ secretion by NPD was markedly reduced in mice exposed to LPS (* p <0.05, n = 6), while the impact was negated when co-incubated with GSH or TAK242 which were similar to control vehicle.

channel open probability and diminished numbers of active channels cannot be attributed to protein degradation or turnover. While chronic activation of redox pathways by LPS would be likely to confer ER stress, UPR or ISR, these mechanisms are unlikely to be the cause of functional changes to the channels exhibited in our study. Furthermore, increased intracellular Cl⁻, shown to trigger an IL-1 β autocrine and positive feedback loop in CF bronchial epithelial cells and ROS-mediated inflammation, [88–90] was observed in a 24–48 h time frame, well outside the window of observed effects in the present study. Yet, it is possible that the changes caused by ROS (carbonylation) affected the function of CFTR, particularly since CFTR protein expression (bands B and C), as well as surface localization, were not altered. GSH, the most abundant cellular thiol antioxidant, critical to maintaining intracellular redox balance and redox-sensitive signaling events abrogated the LPS-induced acquired CFTR dysfunction and subsequent carbonylation of CFTR. Previous studies have shown GSH is chronically low in the fluid that lines the epithelial layer of lung tissue subjected to chronic *Pseudomonas* infection [91,92]. Pulmonary GSH levels are also decreased in CF patients, but intracellular redox potential in CF and CFTR-corrected nasal epithelial cells is normal. Thus, *P. aeruginosa*-derived LPS could be one of the factors responsible for oxidative stress and impairments in GSH status in the airways of CF patients *in vivo*. Importantly, strategies to scavenge oxidative stress in the airways represent an important platform for disease intervention.

Acquired CFTR deficiency contributing to the propagation of chronic infection in CRS differs substantially from prevailing models regarding the pathogenesis of CRS [93–97]. The possibility of dysfunctional Cl⁻ transport in CRS suggests new avenues relevant to the field of rhinology and sinus disease; in particular, LPS decreasing CFTR-mediated transport has important implications for understanding impaired MCT in numerous upper and lower respiratory infectious illnesses. Regardless of the mechanism underlying LPS-mediated CFTR dysfunction, increasing transepithelial Cl⁻ secretion and apical fluid hydration are appealing options for therapeutic intervention, and the evidence for pronounced dysfunction provides an impetus for activating CFTR as a means to promote MCT in individuals with CRS. Furthermore, blunting cellular oxidative stress with ROS scavenger compounds could reverse MCT defects and improve respiratory epithelial health in the setting of early colonization and/or infection. Although this therapeutic approach could have harmful effects in patients by impacting innate immunity, tactics to

utilize topical, inhaled drugs to reduce ROS are already clinically approved for use – in particular, the redox agent and free radical scavenger, N-acetyl cysteine, has been used to remove mucus plugs in CF and other respiratory diseases of mucus obstruction [98,99].

In conclusion, this study demonstrated that pathophysiological concentrations of LPS adversely affect REC CFTR function through the generation of ROS and confer substantial dysfunction to markers of MCT. The major effect of LPS causes potent inhibition to active CFTR Cl⁻ transport and MCT, and thus permits colonization and propagation of infection with *P. aeruginosa* and other GNB in upper and lower airways. While the findings have implications for early colonization and infection with GNB in non-CF airways, LPS is a critical factor that should also be considered in CF airways colonized or recurrently infected with *Pseudomonas*, including the respiratory tract of patients with improved CFTR function due to CFTR modulator therapy. Furthermore, in the setting of chronic GNB infection in non-CF CRS, restoration of impaired CFTR function with CFTR potentiators or ROS scavengers represents a critical and innovative approach to therapy.

5. Funding

This work was supported by the National Institutes of Health (NIH)/National Institutes of Allergy and Infectious disease (K08AI146220-02) to D.Y.C.; NIH/National Institute of Diabetes and Digestive and Kidney Diseases (5P30DK072482-03) to S.M.R.; NIH/National Institute of Environmental Health Sciences (NIEHS) (5U01 ES026458; 3U01 ES026458 03S1; 5U01 ES027697) to S.M.; NIH/ National Heart, Lung, and Blood Institute (NHLBI) (R01HL139876 and R01HL136414) to E.J.S; and NIH/NHLBI (R01 HL133006-05 and K08HL107142-05) to B.A.W.

Author contributions

Do Yeon Cho, M.D. – Conceptualization, Data Curation, Formal Analysis, Funding Acquisition, Investigation, Methodology, Project Administration, Supervision, Validation, Writing – review & editing. Shaoyan Zhang, Ph.D. - Conceptualization, Data Curation, Formal Analysis, Investigation, Methodology, Project Administration, Validation, Writing – review & editing, Ahmed Lazrak, Ph.D. - Data Curation, Formal Analysis, Investigation, Methodology, Writing – review & editing, Daniel Skinner, B.S. - Data Curation, Formal Analysis, Investigation,

Writing – review & editing. Harrison M. Thompson, B.S. - Data Curation, Investigation, Writing – review & editing. Jessica Grayson, M.D. - Data Curation, Formal Analysis, Investigation, Methodology, Project Administration, Writing – review & editing. Purushotham Guroji, Ph.D. - Formal Analysis, Investigation, Writing – review & editing. Saurabh Aggarwal, Ph.D. - Formal Analysis, Investigation, Writing – review & editing. Zsuzsanna Bebok, M.D. - Methodology, Supervision, Project Administration, Validation, Writing – review & editing. Steven M. Rowe, M.D. - Funding Acquisition, Methodology, Project Administration, Supervision, Validation, Writing – review & editing. Sadis Matalon, Ph.D. - Conceptualization, Funding Acquisition, Methodology, Project Administration, Validation, Writing – review & editing. Eric J. Sorscher, M.D. - Conceptualization, Funding Acquisition, Project Administration, Writing – review & editing. Bradford A. Woodworth, M.D., F.A.C.S. - Conceptualization, Data Curation, Formal Analysis, Funding Acquisition, Investigation, Methodology, Project Administration, Resources, Supervision, Visualization, Validation, Writing – original draft.

Declaration of competing interest

The authors declare no competing financial interests.

Acknowledgements

The authors would like to acknowledge John C. Kappes, PhD for permitting use of flag-tagged recombinant CFTR (D519 CFBE-mCMV-CFTR_WT_901FLAG (UAB-corrected sequence) clone # 7).

Appendix A. Supplementary data

Supplementary data to this article can be found online at <https://doi.org/10.1016/j.redox.2021.101998>.

References

- [1] L. Caulley, K. Thavorn, L. Rudmik, C. Cameron, S.J. Kilty, Direct costs of adult chronic rhinosinusitis by using 4 methods of estimation: results of the US Medical Expenditure Panel Survey, *J. Allergy Clin. Immunol.* 136 (6) (Dec 2015) 1517–1522.
- [2] A.S. DeConde, Z.M. Soler, Chronic rhinosinusitis: epidemiology and burden of disease, *Am. J. Rhinol. Allergy* 30 (2) (Mar–Apr 2016) 134–139.
- [3] R.E. Gliklich, R. Metson, The health impact of chronic sinusitis in patients seeking otolaryngologic care, *Otolaryngology-Head Neck Surg : Off. J. Am. Acad. Otolaryngology-Head Neck Surg.* 113 (1) (Jul 1995) 104–109.
- [4] R.R. Orlandi, T.T. Kingdom, T.L. Smith, et al., International consensus statement on allergy and rhinology: rhinosinusitis 2021, *Int. Forum. Allergy. Rhinol* 11 (3) (March 2021) 213–739.
- [5] E. El Rassi, J.C. Mace, T.O. Steele, J.A. Alt, T.L. Smith, Improvements in sleep-related symptoms after endoscopic sinus surgery in patients with chronic rhinosinusitis, *Int. Forum. Allergy. Rhinol* 6 (4) (Apr 2016) 414–422.
- [6] A.C. Chester, R. Sindwani, T.L. Smith, N. Bhattacharyya, Fatigue improvement following endoscopic sinus surgery: a systematic review and meta-analysis, *Laryngoscope* 118 (4) (Apr 2008) 730–739.
- [7] S.M. Rowe, S. Miller, E.J. Sorscher, Cystic fibrosis, *N. Engl. J. Med.* 352 (19) (May 12 2005) 1992–2001.
- [8] J.F. Collawn, S. Matalon, The role of CFTR in transepithelial liquid transport in pig alveolar epithelia, *Am. J. Physiol. Lung Cell Mol. Physiol.* 303 (6) (Sep 15 2012) L489–L491.
- [9] T.K. Karanth, V. Karanth, B.K. Ward, B.A. Woodworth, L. Karanth, Medical interventions for chronic rhinosinusitis in cystic fibrosis, *Cochrane Database Syst. Rev.* 10 (Oct 23 2019), CD012979.
- [10] K.E. Tipirneni, B.A. Woodworth, Medical and surgical advancements in the management of cystic fibrosis chronic rhinosinusitis, *Curr. Otorhinolaryngol. reports* 5 (1) (Mar 2017) 24–34.
- [11] E.A. Illing, B.A. Woodworth, Management of the upper airway in cystic fibrosis, *Curr. Opin. Pulm. Med.* 20 (6) (Nov 2014) 623–631.
- [12] X. Wang, B. Moylan, D.A. Leopold, et al., Mutation in the gene responsible for cystic fibrosis and predisposition to chronic rhinosinusitis in the general population, *JAMA* 284 (14) (Oct 11 2000) 1814–1819.
- [13] A.C. Miller, A.P. Comellas, D.B. Hornick, et al., Cystic fibrosis carriers are at increased risk for a wide range of cystic fibrosis-related conditions, *Proc. Natl. Acad. Sci. U. S. A* 117 (3) (Jan 21 2020) 1621–1627.
- [14] N.A. Cohen, S. Zhang, D.B. Sharp, et al., Cigarette smoke condensate inhibits transepithelial chloride transport and ciliary beat frequency, *Laryngoscope* 119 (11) (Nov 2009) 2269–2274.
- [15] D.P. MacEachran, B.A. Stanton, G.A. O'Toole, Cif is negatively regulated by the TetR family repressor CifR, *Infect. Immun.* 76 (7) (Jul 2008) 3197–3206.
- [16] Z. Bebok, K. Varga, J.K. Hicks, et al., Reactive oxygen nitrogen species decrease cystic fibrosis transmembrane conductance regulator expression and cAMP-mediated Cl⁻ secretion in airway epithelia, *J. Biol. Chem.* 277 (45) (Nov 8 2002) 43041–43049.
- [17] C. Banks, L. Freeman, D.Y. Cho, B.A. Woodworth, Acquired cystic fibrosis transmembrane conductance regulator dysfunction, *World J. Otorhinolaryngol. Head Neck Surg.* 4 (3) (Sep 2018) 193–199.
- [18] K. Asai, S. Haruna, N. Otori, K. Yanagi, M. Fukami, H. Moriyama, Saccharin test of maxillary sinus mucociliary function after endoscopic sinus surgery, *Laryngoscope* 110 (1) (Jan 2000) 117–122.
- [19] K.E. Tipirneni, S. Zhang, D.Y. Cho, et al., Submucosal gland mucus strand velocity is decreased in chronic rhinosinusitis, *Int. Forum. Allergy. Rhinol* 8 (4) (Apr 2018) 509–512.
- [20] A.G. Chiu, J.N. Palmer, B.A. Woodworth, et al., Baby shampoo nasal irrigations for the symptomatic post-functional endoscopic sinus surgery patient, *Am. J. Rhinol.* 22 (1) (Jan–Feb 2008) 34–37.
- [21] D.Y. Cho, D. Skinner, R.C. Hunter, et al., Contribution of short chain fatty acids to the growth of *Pseudomonas aeruginosa* in rhinosinusitis, *Front. Cell. Infect. Microbiol* 10 (2020) 412.
- [22] H.M. Thompson, D.J. Lim, C. Banks, et al., Antibiotic eluting sinus stents, *Laryngoscope invest otolaryngol* 5 (4) (Aug 2020) 598–607.
- [23] J.P. McCormick, H.M. Thompson, D.Y. Cho, B.A. Woodworth, J.W. Grayson, Phenotypes in chronic rhinosinusitis, *Curr. Allergy Asthma Rep.* 20 (7) (May 19 2020) 20.
- [24] D.J. Lim, J. McCormick, D. Skinner, et al., Controlled delivery of ciprofloxacin and ivacaftor via sinus stent in a preclinical model of *Pseudomonas sinusitis*, *Int. Forum. Allergy. Rhinol* 10 (4) (Apr 2020) 481–488.
- [25] D.J. Lim, H.M. Thompson, C.R. Walz, et al., Azithromycin and ciprofloxacin inhibit interleukin-8 secretion without disrupting human sinonasal epithelial integrity in vitro, *Int. Forum. Allergy. Rhinol.* 11 (2) (2021) 136–143.
- [26] D.Y. Cho, D.J. Lim, C. Mackey, et al., Ivacaftor, a cystic fibrosis transmembrane conductance regulator potentiator, enhances ciprofloxacin activity against *Pseudomonas aeruginosa*, *Am. J. Rhinol. Allergy* 33 (2) (Mar 2019) 129–136.
- [27] D.Y. Cho, D.J. Lim, C. Mackey, et al., In-vitro evaluation of a ciprofloxacin- and ivacaftor-coated sinus stent against *Pseudomonas aeruginosa* biofilms, *Int. Forum. Allergy. Rhinol* 9 (5) (May 2019) 486–492.
- [28] D.Y. Cho, D.J. Lim, C. Mackey, et al., Preclinical therapeutic efficacy of the ciprofloxacin-eluting sinus stent for *Pseudomonas aeruginosa* sinusitis, *Int. Forum. Allergy. Rhinol* 8 (4) (Apr 2018) 482–489.
- [29] D.Y. Cho, C. Mackey, W.J. Van Der Pol, et al., Sinus microanatomy and microbiota in a rabbit model of rhinosinusitis, *Front. Cell. Infect. Microbiol* 7 (2017) 540.
- [30] S.A. Fong, A. Drilling, S. Morales, et al., Activity of bacteriophages in removing biofilms of *Pseudomonas aeruginosa* isolates from chronic rhinosinusitis patients, *Front. Cell. Infect. Microbiol* 7 (2017) 418.
- [31] L.L. Lau, J. Jiang, H. Shen, In vivo modulation of T cell responses and protective immunity by TCR antagonism during infection, *J. Immunol.* 174 (12) (Jun 15 2005) 7970–7976.
- [32] Z. Zhang, J.P. Louboutin, D.J. Weiner, J.B. Goldberg, J.M. Wilson, Human airway epithelial cells sense *Pseudomonas aeruginosa* infection via recognition of flagellin by Toll-like receptor 5, *Infect. Immun.* 73 (11) (Nov 2005) 7151–7160.
- [33] R.T. Sadikot, T.S. Blackwell, J.W. Christman, A.S. Prince, Pathogen-host interactions in *Pseudomonas aeruginosa* pneumonia, *Am. J. Respir. Crit. Care Med.* 171 (11) (Jun 1 2005) 1209–1223.
- [34] I. Ghai, S. Ghai, Understanding antibiotic resistance via outer membrane permeability, *Infect. Drug Resist.* 11 (2018) 523–530.
- [35] A.H. Delcour, Outer membrane permeability and antibiotic resistance, *Biochim. Biophys. Acta* 1794 (5) (May 2009) 808–816.
- [36] T.H. Schroeder, M.M. Lee, P.W. Yacono, et al., CFTR is a pattern recognition molecule that extracts *Pseudomonas aeruginosa* LPS from the outer membrane into epithelial cells and activates NF- κ B translocation, *Proc. Natl. Acad. Sci. U. S. A* 99 (10) (May 14 2002) 6907–6912.
- [37] E.G. Cafferata, A.M. Guerrico, O.H. Pivetta, T.A. Santa-Coloma, NF- κ B activation is involved in regulation of cystic fibrosis transmembrane conductance regulator (CFTR) by interleukin-1 β , *J. Biol. Chem.* 276 (18) (May 4 2001) 15441–15444.
- [38] P.M. Farrell, T.B. White, M.S. Howenstine, et al., Diagnosis of cystic fibrosis in screened populations, *J. Pediatr.* 181S (Feb 2017) S33–S44 e32.
- [39] G. Bhargave, B.A. Woodworth, G. Xiong, S.G. Wolfe, M.B. Antunes, N.A. Cohen, Transient receptor potential vanilloid type 4 channel expression in chronic rhinosinusitis, *Am. J. Rhinol.* 22 (1) (Jan–Feb 2008) 7–12.
- [40] F.W. Virgin, C. Azzell, D. Schuster, et al., Exposure to cigarette smoke condensate reduces calcium activated chloride channel transport in primary sinonasal epithelial cultures, *Laryngoscope* 120 (7) (Jul 2010) 1465–1469.
- [41] B.A. Woodworth, M.B. Antunes, G. Bhargave, J.N. Palmer, N.A. Cohen, Murine tracheal and nasal septal epithelium for air-liquid interface cultures: a comparative study, *Am. J. Rhinol.* 21 (5) (Sep–Oct 2007) 533–537.
- [42] M.B. Antunes, B.A. Woodworth, G. Bhargave, et al., Murine nasal septa for respiratory epithelial air-liquid interface cultures, *Biotechniques* 43 (2) (Aug 2007) 195–196, 198, 200 passim.
- [43] B.A. Woodworth, E. Tamashiro, G. Bhargave, N.A. Cohen, J.N. Palmer, An in vitro model of *Pseudomonas aeruginosa* biofilms on viable airway epithelial cell monolayers, *Am. J. Rhinol.* 22 (3) (May–Jun 2008) 235–238.
- [44] S. Zhang, J.A. Fortenberry, N.A. Cohen, E.J. Sorscher, B.A. Woodworth, Comparison of vectorial ion transport in primary murine airway and human

- sinonasal air-liquid interface cultures, models for studies of cystic fibrosis, and other airway diseases, *Am. J. Rhinol. Allergy* 23 (2) (Mar-Apr 2009) 149–152.
- [45] D.C. Gruenert, M. Willems, J.J. Cassiman, R.A. Frizzell, Established cell lines used in cystic fibrosis research, *J. Cyst. Fibros. : Off. J. Eur. Cystic. Fibros. Soc.* 3 (2) (Aug 2004) 191–196.
- [46] N. Dean, N.K. Ranganath, B. Jones, et al., Porcine nasal epithelial cultures for studies of cystic fibrosis sinusitis, *Int. Forum. Allergy. Rhinol* 4 (7) (Jul 2014) 565–570.
- [47] D.Y. Cho, S. Zhang, A. Lazrak, et al., Resveratrol and ivacaftor are additive G551D CFTR-channel potentiators: therapeutic implications for cystic fibrosis sinus disease, *Int. Forum. Allergy. Rhinol* 9 (1) (Jan 2019) 100–105.
- [48] J.D. Londino, A. Lazrak, J.W. Noah, et al., Influenza virus M2 targets cystic fibrosis transmembrane conductance regulator for lysosomal degradation during viral infection, *Faseb. J. : Off. Publ. Fed. Am. Soc. Exp. Biol.* 29 (7) (Jul 2015) 2712–2725.
- [49] A. Lazrak, A. Jurkuvenaite, E.C. Ness, et al., Inter-alpha-inhibitor blocks epithelial sodium channel activation and decreases nasal potential differences in DeltaF508 mice, *Am. J. Respir. Cell Mol. Biol.* 50 (5) (May 2014) 953–962.
- [50] A. Lazrak, A. Jurkuvenaite, L. Chen, et al., Enhancement of alveolar epithelial sodium channel activity with decreased cystic fibrosis transmembrane conductance regulator expression in mouse lung, *Am. J. Physiol. Lung Cell Mol. Physiol.* 301 (4) (Oct 2011) L557–L567.
- [51] V. Bali, A. Lazrak, P. Guroji, S. Matalon, Z. Bebok, Mechanistic approaches to improve correction of the most common disease-causing mutation in cystic fibrosis, *PLoS One* 11 (5) (2016), e0155882.
- [52] K. Varga, R.F. Goldstein, A. Jurkuvenaite, et al., Enhanced cell-surface stability of rescued DeltaF508 cystic fibrosis transmembrane conductance regulator (CFTR) by pharmacological chaperones, *Biochem. J.* 410 (3) (Mar 15 2008) 555–564.
- [53] S. Aggarwal, J.J. DeBerry, I. Ahmad, et al., Heme attenuates beta-endorphin levels in leukocytes of HIV positive individuals with chronic widespread pain, *Redox Biol* 36 (Sep 2020), 101684.
- [54] S. Aggarwal, A. Lam, S. Bolisetty, et al., Heme attenuation ameliorates irritant gas inhalation-induced acute lung injury, *Antioxidants Redox Signal.* 24 (2) (Jan 10 2016) 99–112.
- [55] S. Aggarwal, A. Lazrak, I. Ahmad, et al., Reactive species generated by heme impair alveolar epithelial sodium channel function in acute respiratory distress syndrome, *Redox Biol* 36 (Sep 2020), 101592.
- [56] N.A. Ramella, G.R. Schinella, S.T. Ferreira, et al., Human apolipoprotein A-I natural variants: molecular mechanisms underlying amyloidogenic propensity, *PLoS One* 7 (8) (2012), e43755.
- [57] L. Liu, K.K. Chu, G.H. Houser, et al., Method for quantitative study of airway functional microanatomy using micro-optical coherence tomography, *PLoS One* 8 (1) (2013), e54473.
- [58] H.M. Leung, S.E. Birket, C. Hyun, et al., Intranasal micro-optical coherence tomography imaging for cystic fibrosis studies, *Sci. Transl. Med.* 11 (504) (Aug 7 2019).
- [59] D.Y. Cho, D. Skinner, C. Mackey, et al., Herbal dry extract BNO 1011 improves clinical and mucociliary parameters in a rabbit model of chronic rhinosinusitis, *Int. Forum. Allergy. Rhinol* 9 (6) (Jun 2019) 629–637.
- [60] K.E. Tipirneni, J.W. Grayson, S. Zhang, et al., Assessment of acquired mucociliary clearance defects using micro-optical coherence tomography, *Int. Forum. Allergy. Rhinol* 7 (9) (Sep 2017) 920–925.
- [61] S.E. Birket, K.K. Chu, G.H. Houser, et al., Combination therapy with cystic fibrosis transmembrane conductance regulator modulators augment the airway functional microanatomy, *Am. J. Physiol. Lung Cell Mol. Physiol.* 310 (10) (May 15 2016) L928–L939.
- [62] B.A. Woodworth, Resveratrol ameliorates abnormalities of fluid and electrolyte secretion in a hypoxia-induced model of acquired CFTR deficiency, *Laryngoscope* 125 (7) (Oct 2015) S1–S13.
- [63] N.S. Alexander, N. Hatch, S. Zhang, et al., Resveratrol has salutary effects on mucociliary transport and inflammation in sinonasal epithelium, *Laryngoscope* 121 (6) (Jun 2011) 1313–1319.
- [64] F. Virgin, S. Zhang, D. Schuster, et al., The bioflavonoid compound, sinupret, stimulates transepithelial chloride transport in vitro and in vivo, *Laryngoscope* 120 (5) (May 2010) 1051–1056.
- [65] J.D. Brand, A. Lazrak, J.E. Trombley, et al., Influenza-mediated reduction of lung epithelial ion channel activity leads to dysregulated pulmonary fluid homeostasis, *JCI insight* 3 (20) (Oct 18 2018).
- [66] P. Kumar, A. Nagarajan, P.D. Uchil, Analysis of cell viability by the lactate Dehydrogenase assay, *Cold Spring Harb. Protoc.* (6) (Jun 1 2018).
- [67] S. Zhang, N.K. Ranganath, D. Skinner, et al., Marked repression of CFTR mRNA in the transgenic Cfr(tm1kth) mouse model, *J. Cyst. Fibros. : Off. J. Eur. Cystic. Fibros. Soc.* 13 (3) (May 2014) 351–352.
- [68] C. Azbell, S. Zhang, D. Skinner, J. Fortenberry, E.J. Sorscher, B.A. Woodworth, Hesperidin stimulates cystic fibrosis transmembrane conductance regulator-mediated chloride secretion and ciliary beat frequency in sinonasal epithelium, *Otolaryngology-Head Neck Surg. : Off. J. Am. Acad. Otolaryngology-Head Neck Surg.* 143 (3) (Sep 2010) 397–404.
- [69] S. Zhang, D. Skinner, S.B. Hicks, et al., Sinupret activates CFTR and TMEM16A-dependent transepithelial chloride transport and improves indicators of mucociliary clearance, *PLoS One* 9 (8) (2014), e104090.
- [70] E. Raoust, V. Balloy, I. Garcia-Verdugo, L. Touqui, R. Ramphal, M. Chignard, *Pseudomonas aeruginosa* LPS or flagellin are sufficient to activate TLR-dependent signaling in murine alveolar macrophages and airway epithelial cells, *PLoS One* 4 (10) (Oct 6 2009), e7259.
- [71] P. Wu, D. Ye, D. Zhang, L. Zhang, J. Wan, Q. Pan, Dual effect of 3,4-dihydroxyacetophenone on LPS-induced apoptosis in RAW264.7 cells by modulating the production of TNF-alpha, *J. Huazhong Univ. Sci. Technol. Med. Sci.* 25 (2) (2005) 131–134.
- [72] C. Suzuki, K. Yoshioka, S. Iwamura, H. Hirose, Endotoxin induces delayed ovulation following endocrine aberration during the proestrous phase in Holstein heifers, *Domest. Anim. Endocrinol.* 20 (4) (May 2001) 267–278.
- [73] A.P. Lowe, R.S. Thomas, A.T. Nials, E.J. Kidd, K.J. Broadley, W.R. Ford, LPS exacerbates functional and inflammatory responses to ovalbumin and decreases sensitivity to inhaled fluticasone propionate in a Guinea pig model of asthma, *Br. J. Pharmacol.* 172 (10) (May 2015) 2588–2603.
- [74] C. Porro, S. Di Gioia, T. Trotta, et al., Pro-inflammatory effect of cystic fibrosis sputum microparticles in the murine lung, *J. Cyst. Fibros. : Off. J. Eur. Cystic. Fibros. Soc.* 12 (6) (Dec 2013) 721–728.
- [75] E. Boncoeur, V. Tardif, M.C. Tessier, et al., Modulation of epithelial sodium channel activity by lipopolysaccharide in alveolar type II cells: involvement of purinergic signaling, *Am. J. Physiol. Lung Cell Mol. Physiol.* 298 (3) (Mar 2010) L417–L426.
- [76] S. Zhang, A.C. Blount, C.M. McNicholas, et al., Resveratrol enhances airway surface liquid depth in sinonasal epithelium by increasing cystic fibrosis transmembrane conductance regulator open probability, *PLoS One* 8 (11) (2013), e81589.
- [77] A. Blount, S. Zhang, M. Chestnut, et al., Transepithelial ion transport is suppressed in hypoxic sinonasal epithelium, *Laryngoscope* 121 (9) (Sep 2011) 1929–1934.
- [78] P.A. Sloane, S. Shastry, A. Wilhelm, et al., A pharmacologic approach to acquired cystic fibrosis transmembrane conductance regulator dysfunction in smoking related lung disease, *PLoS One* 7 (6) (2012), e39809.
- [79] S. Matalon, K. Shrestha, M. Kirk, et al., Modification of surfactant protein D by reactive oxygen-nitrogen intermediates is accompanied by loss of aggregating activity, in vitro and in vivo, *Faseb. J. : Off. Publ. Fed. Am. Soc. Exp. Biol.* 23 (5) (May 2009) 1415–1430.
- [80] K.E. Iles, W. Song, D.W. Miller, D.A. Dickinson, S. Matalon, Reactive species and pulmonary edema, *Exp. Rev. Respir. Med.* 3 (5) (Oct 1 2009) 487–496.
- [81] W. Song, S. Matalon, Modulation of alveolar fluid clearance by reactive oxygen-nitrogen intermediates, *Am. J. Physiol. Lung Cell Mol. Physiol.* 293 (4) (Oct 2007) L855–L858.
- [82] S. Matalon, K.M. Hardiman, L. Jain, et al., Regulation of ion channel structure and function by reactive oxygen-nitrogen species, *Am. J. Physiol. Lung Cell Mol. Physiol.* 285 (6) (Dec 2003) L1184–L1189.
- [83] T. Jilling, I.Y. Haddad, S.H. Cheng, S. Matalon, Nitric oxide inhibits heterologous CFTR expression in polarized epithelial cells, *Am. J. Physiol.* 277 (1) (Jul 1999) L89–L96.
- [84] W. Wang, C. Oliva, G. Li, A. Holmgren, C.H. Lillig, K.L. Kirk, Reversible silencing of CFTR chloride channels by glutathionylation, *J. Gen. Physiol.* 125 (2) (Feb 2005) 127–141.
- [85] E.F. van 't Wout, A. van Schadewijk, R. van Bortel, et al., Virulence factors of *Pseudomonas aeruginosa* induce both the unfolded protein and integrated stress responses in airway epithelial cells, *PLoS Pathog* 11 (6) (Jun 2015), e1004946.
- [86] A. Rab, R. Bartoszewski, A. Jurkuvenaite, J. Wakefield, J.F. Collawn, Z. Bebok, Endoplasmic reticulum stress and the unfolded protein response regulate genomic cystic fibrosis transmembrane conductance regulator expression, *Am. J. Physiol. Cell Physiol.* 292 (2) (Feb 2007) C756–C766.
- [87] R. Bartoszewski, A. Rab, G. Twitty, et al., The mechanism of cystic fibrosis transmembrane conductance regulator transcriptional repression during the unfolded protein response, *J. Biol. Chem.* 283 (18) (May 2 2008) 12154–12165.
- [88] M.M. Massip-Copiz, M. Clazure, A.G. Valdivieso, T.A. Santa-Coloma, CFTR impairment upregulates c-Src activity through IL-1beta autocrine signaling, *Arch. Biochem. Biophys.* 616 (Feb 15 2017) 1–12.
- [89] M. Clazure, A.G. Valdivieso, M.M. Massip-Copiz, et al., Intracellular chloride concentration changes modulate IL-1beta expression and secretion in human bronchial epithelial cultured cells, *J. Cell. Biochem.* 118 (8) (Aug 2017) 2131–2140.
- [90] M. Clazure, A.G. Valdivieso, M.M. Massip-Copiz, G. Schulman, M.L. Teiber, T.A. Santa-Coloma, Disruption of interleukin-1beta autocrine signaling rescues complex I activity and improves ROS levels in immortalized epithelial cells with impaired cystic fibrosis transmembrane conductance regulator (CFTR) function, *PLoS One* 9 (6) (2014), e99257.
- [91] V.M. Hudson, Rethinking cystic fibrosis pathology: the critical role of abnormal reduced glutathione (GSH) transport caused by CFTR mutation, *Free Radical Biol. Med.* 30 (12) (Jun 15 2001) 1440–1461.
- [92] L. Gao, K.J. Kim, J.R. Yankaskas, H.J. Forman, Abnormal glutathione transport in cystic fibrosis airway epithelia, *Am. J. Physiol.* 277 (1) (Jul 1999) L113–L118.
- [93] R.C. Kern, D.B. Conley, W. Walsh, et al., Perspectives on the etiology of chronic rhinosinusitis: an immune barrier hypothesis, *Am. J. Rhinol.* 22 (6) (Nov-Dec 2008) 549–559.
- [94] R.P. Schleimer, A. Kato, A. Peters, et al., Epithelium, inflammation, and immunity in the upper airways of humans: studies in chronic rhinosinusitis, *Proc. Am. Thorac. Soc.* 6 (3) (May 1 2009) 288–294.
- [95] J.M. Bernstein, M. Ballow, P.M. Schlievert, G. Rich, C. Allen, D. Dryja, A superantigen hypothesis for the pathogenesis of chronic hyperplastic sinusitis with massive nasal polyposis, *Am. J. Rhinol.* 17 (6) (Nov-Dec 2003) 321–326.
- [96] J.R. Perloff, J.N. Palmer, Evidence of bacterial biofilms in a rabbit model of sinusitis, *Am. J. Rhinol.* 19 (1) (Jan-Feb 2005) 1–6.
- [97] A.N. Khalid, B.A. Woodworth, A. Prince, et al., Physiologic alterations in the murine model after nasal fungal antigenic exposure, *Otolaryngology-Head Neck*

- Surg : Off. J.Am. Acad. Otolaryngology-Head Neck Surg. 139 (5) (Nov 2008) 695–701.
- [98] M.M. Bridgeman, M. Marsden, C. Selby, D. Morrison, W. MacNee, Effect of N-acetyl cysteine on the concentrations of thiols in plasma, bronchoalveolar lavage fluid, and lung tissue, *Thorax* 49 (7) (Jul 1994) 670–675.
- [99] J. Schreiber, B. Bohnsteen, W. Rosahl, Influence of mucolytic therapy on respiratory mechanics in patients with chronic obstructive pulmonary disease, *Eur. J. Med. Res.* 7 (3) (Mar 28 2002) 98–102.